OAK RIDGE NATIONAL LABORATORY LIBRARIES
3 4456 0576319 9

DATE ISSUED NOV 3 1980

ORNL/TM-7438/V1

800630

ornl

OAK
RIDGE
NATIONAL
LABORATORY

UNION
CARBIDE

Ocean Thermal Energy Conversion Gas Desorption Studies

VOL. 1. DESIGN OF EXPERIMENTS

A. Golshani
F. C. Chen

OPERATED BY
UNION CARBIDE CORPORATION
FOR THE UNITED STATES
DEPARTMENT OF ENERGY

Printed in the United States of America. Available from
National Technical Information Service
U.S. Department of Commerce
5285 Port Royal Road, Springfield, Virginia 22161
NTIS price codes—Printed Copy: A04; Microfiche A01

This report was prepared as an account of work sponsored by an agency of the United States Government. Neither the United States Government nor any agency thereof, nor any of their employees, makes any warranty, express or implied, or assumes any legal liability or responsibility for the accuracy, completeness, or usefulness of any information, apparatus, product, or process disclosed, or represents that its use would not infringe privately owned rights. Reference herein to any specific commercial product, process, or service by trade name, trademark, manufacturer, or otherwise, does not necessarily constitute or imply its endorsement, recommendation, or favoring by the United States Government or any agency thereof. The views and opinions of authors expressed herein do not necessarily state or reflect those of the United States Government or any agency thereof.

ORNL/TM-7438/V1
Dist. Category UC-64

Contract No. W-7405-eng-26

16

OCEAN THERMAL ENERGY CONVERSION GAS DESORPTION STUDIES

Vol. 1. Design of Experiments

A. Golshani 16
Engineering Technology Division

F. C. Chen 15
Energy Division

Date Published - October 1980

NOTICE This document contains information of a preliminary nature. It is subject to revision or correction and therefore does not represent a final report.

Prepared for the
Ocean Systems Branch
Division of Central Solar Technology

Prepared by the
OAK RIDGE NATIONAL LABORATORY
Oak Ridge, Tennessee 37830
operated by
UNION CARBIDE CORPORATION
for the
DEPARTMENT OF ENERGY

CONTENTS

Page

ACKNOWLEDGMENTS v

ABSTRACT 1

1. INTRODUCTION 1

2. PREVIOUS WORK 6

2.1 Gas Desorption 6

2.2 Vacuum Deaeration Studies 7

3. TEST LOOP DESIGN 11

3.1 Test Facility 12

3.2 Test Scheme 15

3.3 Instrumentation 18

3.4 Vacuum Keeping 19

3.5 Air Leakage 20

4. ANALYSIS 21

4.1 Basic Design of Vacuum Desorber 21

4.2 Principles of Vacuum Degasification in a Packed Column ... 21

4.2.1 Solubility of gases in a liquid (Henry's law) 24

4.2.2 Dalton's law 25

4.3 Mass Transfer Fundamentals 25

4.4 Development of Transfer Unit 26

5. RESULTS OF INITIAL TESTS 28

6. PROBLEMS AND UNCERTAINTIES 34

6.1 Operational Factors 34

6.2 Measurement Factors 35

7. CONCLUSIONS 36

8. NOMENCLATURE 40

REFERENCES 42

APPENDIX 45

ACKNOWLEDGMENTS

This investigation was performed at the Oak Ridge National Laboratory (ORNL), operated by Union Carbide Corporation for the Department of Energy (DOE). The study was a part of the general program of the Ocean Systems Branch being carried out by ORNL for the DOE Division of Central Solar Technology.

The authors wish to express their appreciation for the assistance of many ORNL staff members, particularly D. M. Eissenberg, H. W. Hoffman, and J. W. Michel for their helpful suggestions throughout the program and R. L. Linkous (project technician) for operating the test equipment and collecting data.

OCEAN THERMAL ENERGY CONVERSION GAS DESORPTION STUDIES

Vol. 1. Design of Experiments

A. Golshani F. C. Chen

ABSTRACT

Seawater deaeration is a process affecting almost all proposed Ocean Thermal Energy Conversion (OTEC) open-cycle power systems. If the noncondensable dissolved air is not removed from a power system, it will accumulate in the condenser, reduce the effectiveness of condensation, and result in deterioration of system performance. A gas desorption study is being conducted at Oak Ridge National Laboratory (ORNL) with the goal of mitigating these effects; this study is designed to investigate the vacuum deaeration process for low-temperature OTEC conditions where conventional steam stripping deaeration may not be applicable.

The first in a series describing the ORNL studies, this report (1) considers the design of experiments and discusses theories of gas desorption, (2) reviews previous relevant studies, (3) describes the design of a gas desorption test loop, and (4) presents the test plan for achieving program objectives. Results of the first series of verification tests and the uncertainties encountered are also discussed.

A packed column was employed in these verification tests and test data generally behaved as in previous similar studies. Results expressed as the height of transfer unit (HTU) can be correlated with the liquid flow rate by HTU = $4.93L^{0.25}$. End effects were appreciable for the vacuum deaeration system, and a correlation of them to applied vacuum pressure was derived.

---

1. INTRODUCTION

Solar thermal energy stored in the form of heat between the upper and the lower part of the world's tropical oceans can be utilized for power generation. The Department of Energy (DOE) organized the Ocean Thermal Energy Conversion (OTEC) program in 1974 to develop means for exploiting this renewable resource. Analysis suggests that OTEC is far superior to fossil and nuclear options in terms of net energy ratio and is less effective than hydroelectric and geothermal.[1] Power cycle concepts conceived as possible means of harnessing the ocean thermal energy

source include closed, open (e.g., Claude), and various lift cycles. Besides the closed cycle, in which a low boiling point secondary working fluid is employed in a Rankine cycle for power generation, the other OTEC cycle concepts may be generically considered as open cycles. In the open cycles, including the Claude and lift cycles, seawater only is the working fluid for power generation.

While the OTEC closed-cycle power system closely resembles conventional power generation cycles, the open cycle, with its elimination of a secondary working fluid, is conceptually simpler. Though the OTEC open cycle is still in the engineering development and/or scientific feasibility stages, feasibility studies[2-5] have projected that the Claude cycle could be as cost competitive as the closed cycle; the lift cycles promise even better economics.

In OTEC open-cycle systems, a small amount of warm seawater is flashed into steam that in turn becomes the working medium for converting the thermal energy into mechanical work. In a Claude cycle, steam expands in a vapor turbine to produce shaft work; in lift cycles, however, steam expands in vertical tubes to lift liquid water to a higher potential energy state. The liquid water separated from the expanding vapor goes through a hydraulic turbine to produce shaft work. The expanding steam is condensed to create low pressure and to maintain a proper pressure gradient in the system for sustained power generation.

Natural seawater contains many different species of dissolved gases. Nitrogen and oxygen constitute the bulk of these gases, but measurable amounts of argon and free carbon dioxide are also present and will be released during the flashing process. If these noncondensable gases are not removed from the condenser, they will accumulate there, build up the condenser pressure, reduce the system pressure gradient, and affect the rate of power generation.

To maintain a uniform power generation rate, the noncondensable gases accumulated from seawater must be removed continuously from the power system by deaeration. Two deaeration options have been proposed in the previous open-cycle system studies. G. Claude employed a predeaeration process in his open-cycle plant, in which dissolved gases were removed from

the warm seawater stream before they reached the flash evaporator. In the Colorado School of Mines open-cycle power system, a postdeaeration process was proposed in which the dissolved gases accumulated during the flash process were removed at the condenser along with any other system air leakages.

The advantage of the predeaeration process is that the deaeration occurs above the saturation vapor pressure of the seawater. Less pumping power is required to eject the noncondensable gases to the atmosphere, but additional system components, such as deaerators and compressors, are needed. Additional hydraulic head is needed to operate the deaerators. In the postdeaeration system, the deaeration occurs at the condenser, where the system pressure is the lowest. More parasitic power is required to remove the noncondensable gases. Although the deaerator is not needed in the postdeaeration system, more heat transfer surface area is required to compensate for the noncondensable gas effect upon condensation phenomena.

Results of preliminary economic analysis based on conceptual designs of the two deaeration options were compared in a recent open-cycle power system design study by Westinghouse;[2] the results are shown in Table 1. The capital cost is less for the predeaeration option, but the parasitic power loss is more than that of the postdeaeration option.

In the conceptual design analysis, a commercially available packed column vacuum deaerator was selected for the predeaeration system. It was designed to operate at 6.89 kPa (1 psia) with 80% stage effectiveness; the column was packed with 1.22 m (4 ft) of 5.1-cm (2-in.) Raschig rings and required an operating head of 2.71 m (8.9 ft). At the warm seawater flow rate for which the mechanism was designed, the deaerator hydraulic power loss would be 4.68 MW, which represented 63% of the total operating power requirement of the predeaeration process.

In an open-cycle system, deaeration is needed to avoid excessive condenser pressure build-up. A highly efficient predeaeration process is desirable but is not critical for the OTEC power generation. In desalination applications, highly effective predeaeration is essential to avoid

Table 1. Comparison of OTEC deaerator cost and power[a]

Item	Option 1: Predeaeration			Option 2: Postdeaeration		
	Flows and ratios [kg/h (lb/h)]	Cost ($ × 10^6)	MW	Flows and ratios [kg/h (lb/h)]	Cost ($ × 10^6)	MW
Vacuum deaerator, p = 6.89 kPa (1 psia), 80% efficiency		2.84	4.68			
Air removed	6.03×10^3 (13.3×10^3)					
Steam removed	3.63×10^3 (8.0×10^3)					
Steam-air ratio	0.6					
Air removal equipment		2.17	1.3			
Air to condenser [add 1.8×10^3 kg/h (4000 lb/h) leakage]	3.58×10^3 (7.9×10^3)			9.8×10^3 (21.6×10^3)		
Condenser air removal equipment		3.51	1.49		9.6	4.1
Condenser inlet steam-air ratio	547			200		
Condenser area increase, %	40			48		
Condenser cost correction					0.98	
Totals		8.52	7.47		10.58	4.1

[a]Conditions: Open cycle power system
Warm seawater flow = 4.53×10^8 kg/h (1×10^9 lb_m/h)
Surface condenser
Axial compressors
Condenser exit steam-air ratio — 4.0
Condenser saturation temperature — 7.78°C (46°F)
Condenser cost — $12.26 × 10^6

corrosion and scale buildup (99.93% oxgyen and 99% carbon dioxide capability is required); a deaerator design with 80% removal was found sufficient in the Westinghouse study.

Although low-head-loss deaerators are not readily available, many state-of-the-art vacuum deaeration concepts may conceivably be developed to fit the particular OTEC needs where low operating power is more critical than high efficiency. Falling films, rotating disk sprays, and shallow trays with turbulent promoters are among the advanced vacuum deaeration concepts that may find application in OTEC. Utilizing the seawater intake pipe for predeaeration is another promising option; although this was proposed in the original Claude open-cycle power design, the effectiveness of the concept has not been investigated.

The objective of this gas desorption study is thus to investigate the technical feasibility of various design concepts of vacuum deaeration at laboratory scale so that low-head-loss deaerators with reasonable cost may be developed for OTEC applications. Performance screening to identify promising designs will be conducted in a small gas desorption loop. Detailed characterization of the best of these deaerator designs and development of a recommended device are left to other phases of the overall OTEC effort.

This first in a series of planned reports documenting these deaerator screening experiments (1) reviews relevant previous efforts, (2) describes the test loop design, (3) discusses operation and analysis procedures, and (4) presents results (including problems and uncertainties) and conclusions from an initial test series.

2. PREVIOUS WORK

2.1 Gas Desorption Studies

Gas desorption from water is a mass transfer phenomenon. Like any transfer process, the movement of dissolved gas in the liquid phase is driven by the overall available concentration gradient across the interphase and is retarded by diffusional and interfacial resistances in and between the phases. The rate of gas desorption in a device can be increased for gradient differences for a given concentration either by reducing the diffusional and interfacial resistances or by increasing the available surface area. Falling film configuration is an example of a gas desorption device in which high mass transfer coefficient is maintained by reducing the liquid film thickness. Steam or foreign gas stripping is usually used in gas desorption operations to maintain high overall partial pressure differences when the column is operated at higher total pressure. Increasing the flow turbulence level by dynamic agitation and by static turbulent promoters can reduce diffusional and interfacial resistances. The use of packing increases the interfacial area.

Many gas desorption/absorption studies have investigated the effect of controlling factors upon mass transfer with the goal of deriving or verifying theoretical predictive equations. Thus, Emmert and Pigford[6] (1954), Lynn et al.[7] (1955), and Lamourella and Sandall[8] (1972) studied gas desorption/absorption in falling film and wetted-wall columns. The data obtained were compared with such theoretical mass transfer rate models as Lewis and Whitman's stagnant film theory,[9] Higbie's penetration theory,[10] Danckwerts' surface renewal theory,[11] and Levich's eddy diffusivity theory.[12] A few combinations of penetration-surface-renewal and film-penetration theories were also developed to fit and interpret the diversified experimental results.

The mass transfer coefficient k_L (m/h or ft/h) is linearly proportional to the molecular diffusion coefficient D (m^2/h or ft^2/h) in the stagnant film theory and is proportional to the square root of D in the penetration and surface-renewal theories. Among the other theories, k_L

was correlated with D to the nth power for values of n lying between 0.50 and 0.75, depending on the fluid dynamic conditions of the experiments.

The performance of a gas desorption device may involve two or more means of maintaining a high concentration gradient: (1) steam stripping and/or (2) reducing diffusional resistance and extended interphase area by using packed columns and spray towers. However, the combination of these effects and the complicated geometry make theoretical analysis difficult. In Sherwood and Holloways's study[13] of gas desorption in a packed column with air stripping and in many later similar studies, simple theoretical models were unable to depict the gas desorption phenomenon. Concepts of liquid and gas film coefficients (k_La, k_ga), HTU, and number of transfer unit (NTU) were introduced and used to correlate the data empirically with various nondimensional parameters.

A modified version of the empirical correlation formula proposed by Sherwood and Holloway[13] is commonly used in gas desorption studies:

$$k_La/D = \alpha(L/\mu)^y(\mu/\rho D)^s$$

and

$$(HTU)_L = \beta(L/\mu)^z(\mu/\rho D)^r .$$

These are derived from the dimensionless form, but an unknown factor having the dimension of length is omitted in the left side and in the first group on the right in both equations. Because of this omission the equation is not dimensionless, and the proportionality constants α and β may be expected to vary with the nature of the packing material and the units employed.

2.2 Vacuum Deaeration Studies

Degasification is a major mass transfer in industrial unit operation. Practical applications vary from degassing of petrochemicals and industrial fluids to deaeration of boiler feed water and potable liquids. Many applications-oriented degassing studies can be found in the literature. Because of the unique OTEC conditions, only those studies involving vacuum deaeration and seawater applications are of relevance to this

investigation; the studies include Knoedler and Bonilla[14] (1954) on packed-column deaeration, Chambers[15] (1959) on seawater spray deaeration, Eissenberg's review[16] (1972) of the performance of deaerators in desalination pilot plants, and the vacuum degassing analysis by Rasguin et al.[17] (1977).

Knoedler and Bonilla investigated vacuum degasification of water in a packed column. A closed test loop was constructed, and oxygen was used as the solute gas. Water enriched with oxygen was pumped into the top of a packed-column test section and directed to a liquid distributor through a screen covered with a holding plate. Water entered the packed column section through distributor orifices. The desorption of oxygen took place in a 15.24-cm-diam (6-in.) column filled with 61 cm (2 ft) of Stedman triangular packing. The evolved oxygen in the test section flowed countercurrently through four vapor risers that penetrated the distributor section and was ejected to the atmosphere by a vacuum pump. The degassed water went through the main circulating pump, was again enriched with oxygen in the absorber, and was returned to the test column. The packing heights were varied from 0 to 61 cm (2 ft), water temperature from 11.11 to 44.45°C (52 to 112°F), liquid rate from 16.6×10^3 to 63.5×10^3 kg/(h·m^2) (3,400 to 13,000 lb/h·ft^2), noncondensable gas pressure from 0.135 to 12.5 kPa (0.04 to 3.7 in. Hg), and concentration of oxygen in the incoming liquid from 3 to 12.7 ppm by weight.

Column flooding was observed when the liquid flow rate was about 73.23×10^3 kg/(h·m^2) [15,000 lb/(h·ft^2)]; and mass transfer resistance was liquid-side controlled. The liquid film coefficient for the packing depended only on liquid flow rate and not on packing height, oxygen concentration, gas pressure, or temperature. Knoedler and Bonilla also observed that end effects were appreciable and depended primarily on temperature. Below the loading point, their vacuum deaeration results could be expressed by the following correlations:

$$\mathrm{HTU} = 1.478\ (L)^{0.3} \tag{2.1}$$

and

$$\frac{k_L a}{D} = 48.85 \times 10^3\ (L)^{0.77}\ (\mu/\rho D)^{0.53}\ . \tag{2.2}$$

A spray-type vacuum deaeration in connection with seawater desalination was investigated by Chambers.[15] A flow schematic of his deaeration test loop is shown in Fig. 1. The deaeration of seawater took place in a 3.66-m-diam (12-ft) hemispherical vacuum chamber. Aerated water was dispersed in the vacuum chamber through twenty 2.58-cm-diam (1-1/64-in.) hollow-cone spray nozzles. The water level in the vacuum chamber bottom was maintained constant at 76.2 cm (30 in.) below the nozzle outlets. The average cross-sectional area between nozzles and water level was 9.75 m^2 (105 ft^2). Tests were made at five water temperatures from 26.67 to 48.9°C (80 to 120°F) in ten intervals and over a pressure range extending from atmospheric pressure to water saturation pressures corresponding to the water temperature of the test. A fixed water flow rate of 31.55 liters/s (500 gpm) was used in the tests.

In Chambers' experiments, air was used as the solute gas with only the dissolved oxygen concentration measured by Winkler titration. Assumptions had to be made as to the rate of release of nitrogen in determining the performance of the vacuum deaerator, since oxygen and nitrogen are

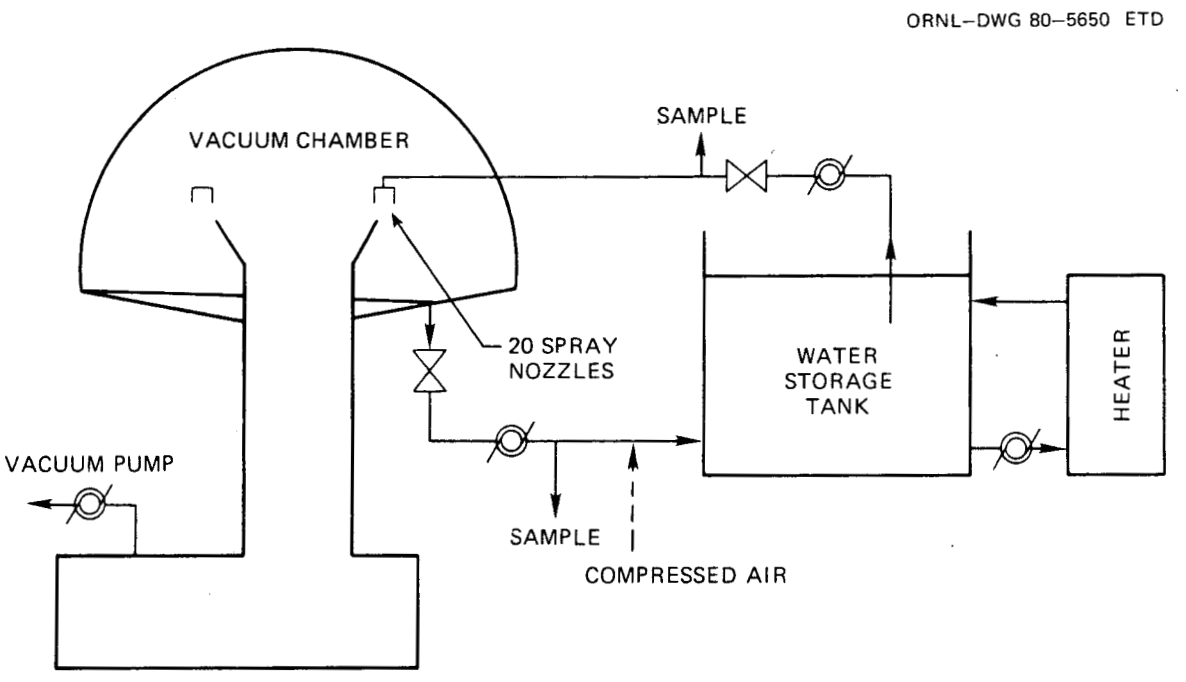

Fig. 1. Schematic flow diagram of a spray deaeration test system.

both sparsely soluble in water. The dissolved air content in the water at reduced pressures was computed from the dissolved oxygen measurements by using Henry's law of gas dissolution and Dalton's law of partial pressure for oxygen and nitrogen. Chambers[15] found that this method was satisfactory for predicting the vacuum deaerator performance and reported that the HTU for the spray-type vacuum deaerator tested in his experiment varied from 21.3 to 45.7 cm (0.7 to 1.5 ft). His data showed that the value of HTU approached 45.7 cm (1.5 ft) as the pressure in the vacuum chamber was reduced. No correlation between HTU and vacuum pressure was presented.

Eissenberg[16] (1972) has reviewed the operating experience of vacuum deaerators for seawater distillation plants; these data came from tests at plant facilities in San Diego, California; Freeport, Texas; Wrightsville Beach, North Carolina; and Oak Ridge, Tennessee. Because of the stringent degassing requirement for desalination plants, steam stripping was used. In order to achieve high rates of desorption, a combination of flashing feed, spray nozzles, and packed or tray columns was employed to increase the interphase area and mass transfer coefficient. Eissenberg concluded that satisfactory deaerators for desalination plants could be designed using one or more mechanisms but that further experimental work was required to optimize costs and to design full-scale units.

Rasquim, Lynn, and Hanson[17] (1977) studied various methods of dissolved air removal from water in packed columns through mathematical modeling. They studied cases of both countercurrent desorption (with and without steam stripping) and cocurrent gas desorption. They found that the gas removal rate in a two-stage cocurrent column was comparable to the countercurrent column with steam stripping and that less energy was consumed.

3. TEST LOOP DESIGN

The ORNL gas desorption test loop consists of water storage tank, gas removal system, liquid recirculating system, and a desorption test section. A schematic of the gas desorption system, including temperature, pressure, and oxygen measuring instrumentation in addition to the air absorption unit, is shown in Figs. 2 and 3. The desorption column is constructed of Plexiglas; all other equipment in the system is made of stainless steel or corrosion-resistant materials.

The preliminary specifications of the gas desorption test loop have been established as follows:

Operating water flow range	0.3–1.89 liters/s (5–30 gpm)
Operating temperature	10–26.7°C (50–80°F)
Loop design pressure	308 kPa (30 psig)
Desorption vacuum pressure range	3.45–34.5 kPa (0.5–5 psia)

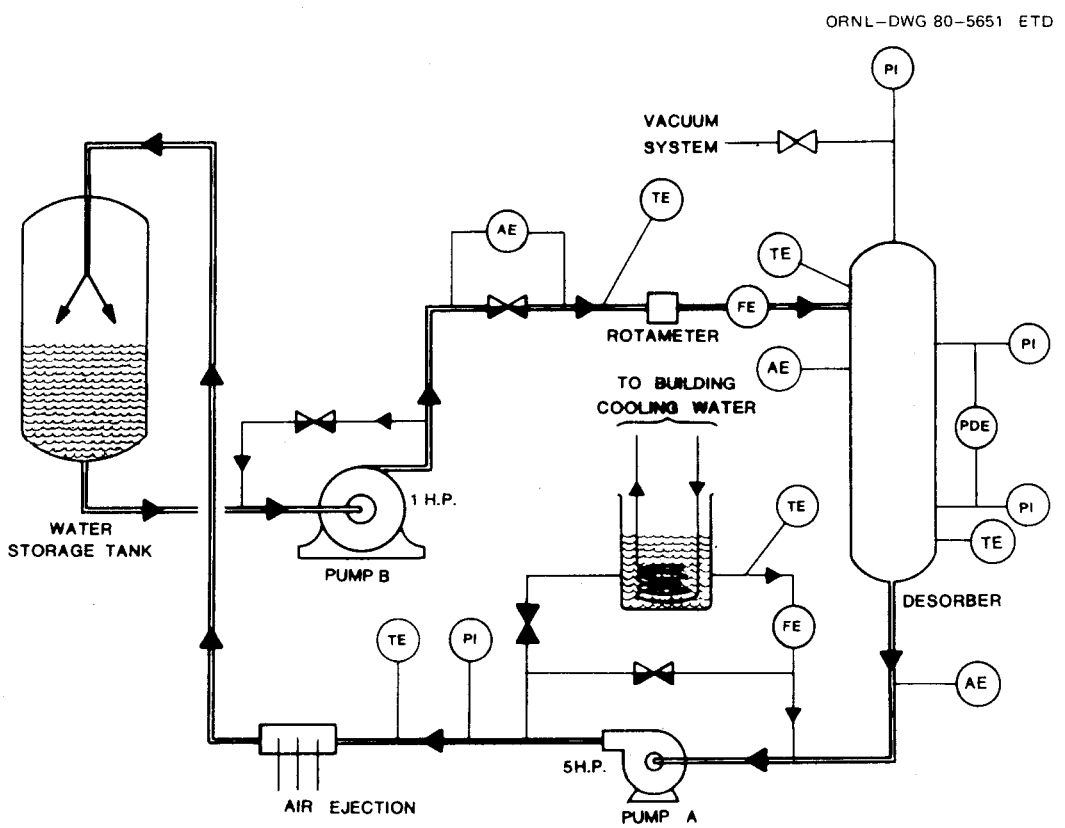

Fig. 2. Gas desorption test loop.

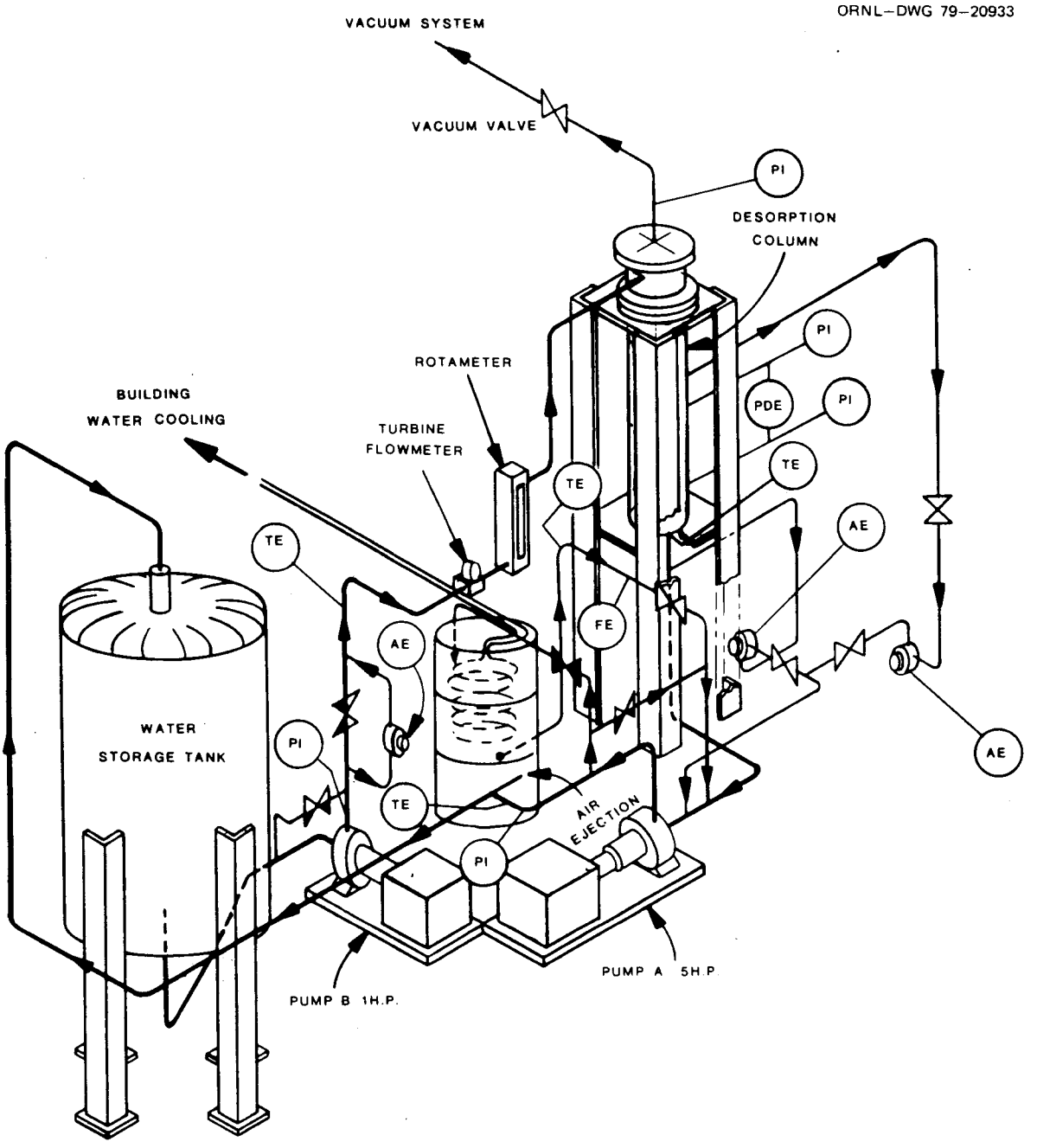

Fig. 3. Gas desorption test facility.

3.1 Test Facility

The major components of the test facility are described as follows.

1. Desorption column. Deaeration takes place in the section labeled "desorption column" in Fig. 3. Its diameter is 30.48 cm (1 ft), and the

total height is 1.83 m (6 ft). Below the packing support is a well that serves as a reservoir for deaerated water. Figure 4 shows a cut-away view of the vertical packed column test section. At the top of the test section is a removable distributor plate located 10.2 cm (4 in.) above the packing. The plate contains 11 orifices for the liquid flow and 4 vapor risers which project upward so that the water will not overflow through the risers. The pressure in the gas desorption system is measured at four locations by mercury manometers: in the vapor line, above the distributor plate, and just above and below the packing. Thermistors are used to measure the temperature of the fluid in the test section.

2. Gas removal system. A 10.2-cm-diam (4-in.) steel line followed by a 15.24-cm-diam (6-in.) pipe connects the top of the desorption column to the vacuum equipment. An existing two-stage steam-jet ejector in the building is employed to serve as the vacuum source. It has a nameplate capacity of removing 13.6 kg/h (30 lb/h) of water vapor and 1.36 kg/h (3 lb/h) of air at 1.35 kPa abs (0.4 in. Hg abs). The vacuum pressure is controlled by means of a vacuum pressure regulator. A small amount of air must be bled into the vacuum piping system to obtain satisfactory control of the vacuum pressure under varying test conditions.

3. Dissolved oxygen sampling. Oxygen analyzers at three locations measure the dissolved oxygen in the liquid. Oxygen sensor 1 measures the oxygen of the water flowing into the desorption column. Sensors 2 and 3 measure the oxygen below the distributor plate and the main discharge line from the desorption column respectively. The oxygen analyzers installed are Beckman Model 7002 Oxygen Monitors. Direct dissolved oxygen concentration readings can be obtained from these analyzers, and they are also supplemented by Wrinkler's wet titration of liquid samples for calibration and verification.

4. Liquid recirculating system. The deaerated water leaving the test section flows through a 10.2-cm (4-in.) stainless steel pipe to a 3.73-kW (5-hp) centrifugal pump. This pump forces the water to flow through the air ejection unit (where compressed air is injected into the water flow so that it can be enriched with dissolved air) and the water storage tank. A side stream from the pump discharge flows through a 3.81-cm (1.5-in.) pipe and branches into two loops. The first loop is a

ORNL-DWG 79-20932

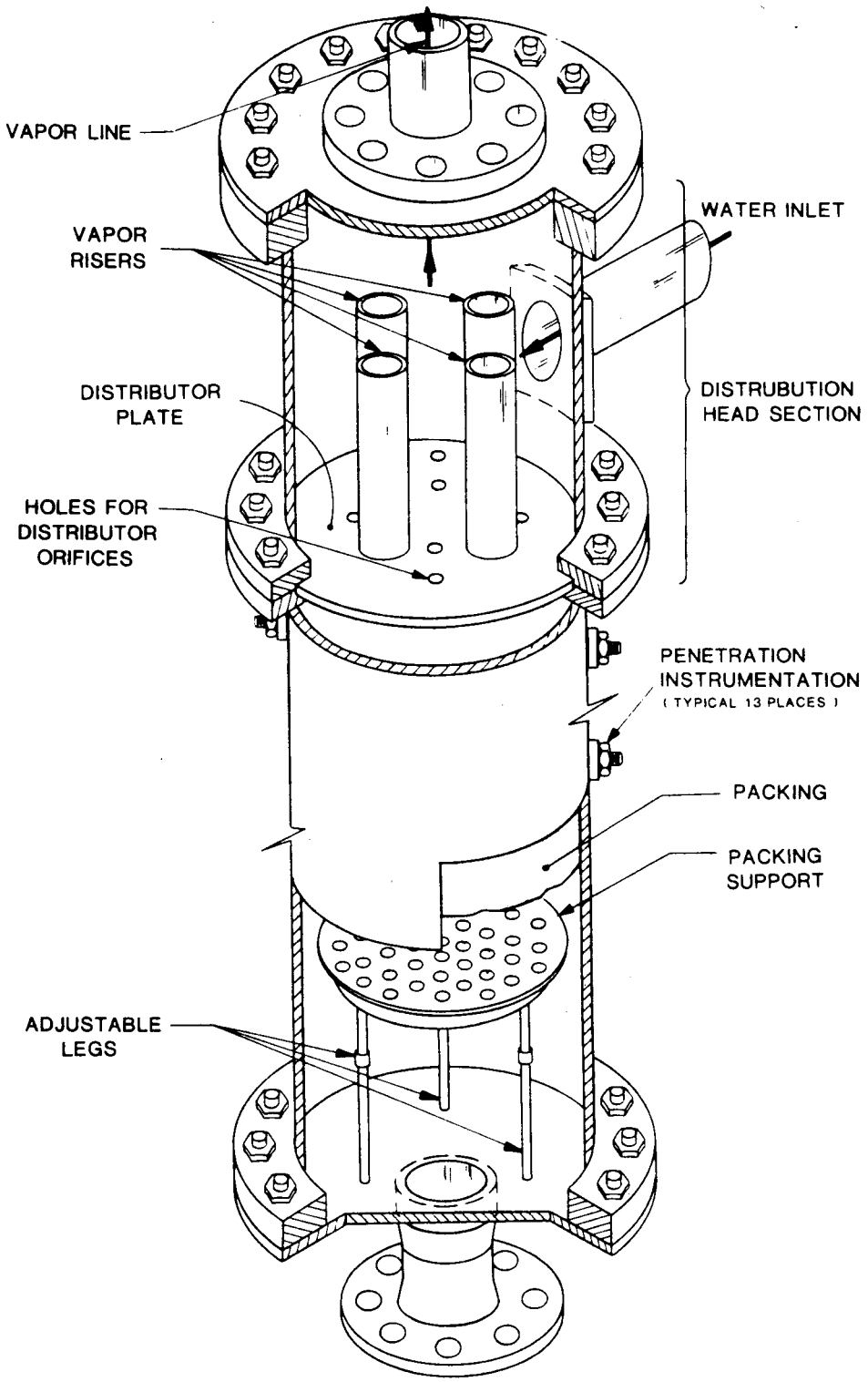

Fig. 4. Desorber test section.

bypass around the pump for proper flow control. The flow rate through the water storage tank is controlled by adjusting the valve across the bypass line. The second loop is for system cooling. It is presently connected to a 208-liter (55-gal) drum where excess heat (such as that generated by the pump) is removed through a heat exchange using the buildings cooling water.

The aerated water leaving the water storage tank flows through a 7.62-cm (3-in.) pipe to a 1.12-kW (1.5-hp) centrifugal pump. The main stream of water flows through the oxygen analyzer bypass valve, turbine flowmeter, and rotameter before entering the desorption test column. The flow rate through the desorption column can also be controlled by adjusting the valve across the bypass line around the 1.12-kW (1.5-hp) pump.

3.2 Test Scheme

Two possible geometrical configurations, vertical and horizontal, are proposed to be tested for water desorption. The first to be considered is the vertical configuration. Many different deaeration concepts can be tested in a vertical column that contains various packings, falling film, and spray. A Raschig-ring packing was tested first, and data obtained were used to verify the loop performance, since relevant data for this kind of packing are available. As the characteristics of the test loop performance are investigated, tests with Pall rings and with falling film and spray concepts shown in Fig. 5 will be followed.

The idea of horizontal desorption configurations is relatively new. There has been no previous investigation on the design or feasibility of horizontal columns. Figure 6 shows the proposed configurations of horizontal arrangements. The performance of channel level—baffled feed, channel sloped—bottom feed, channel stepped—baffled feed, and any additional innovative design configurations will be explored in the horizontal arrangement.

The proposed gas desorption test is intended to test various deaerator design configurations and to identify the promising ones for OTEC application. Only the promising deaerator configurations will be subject

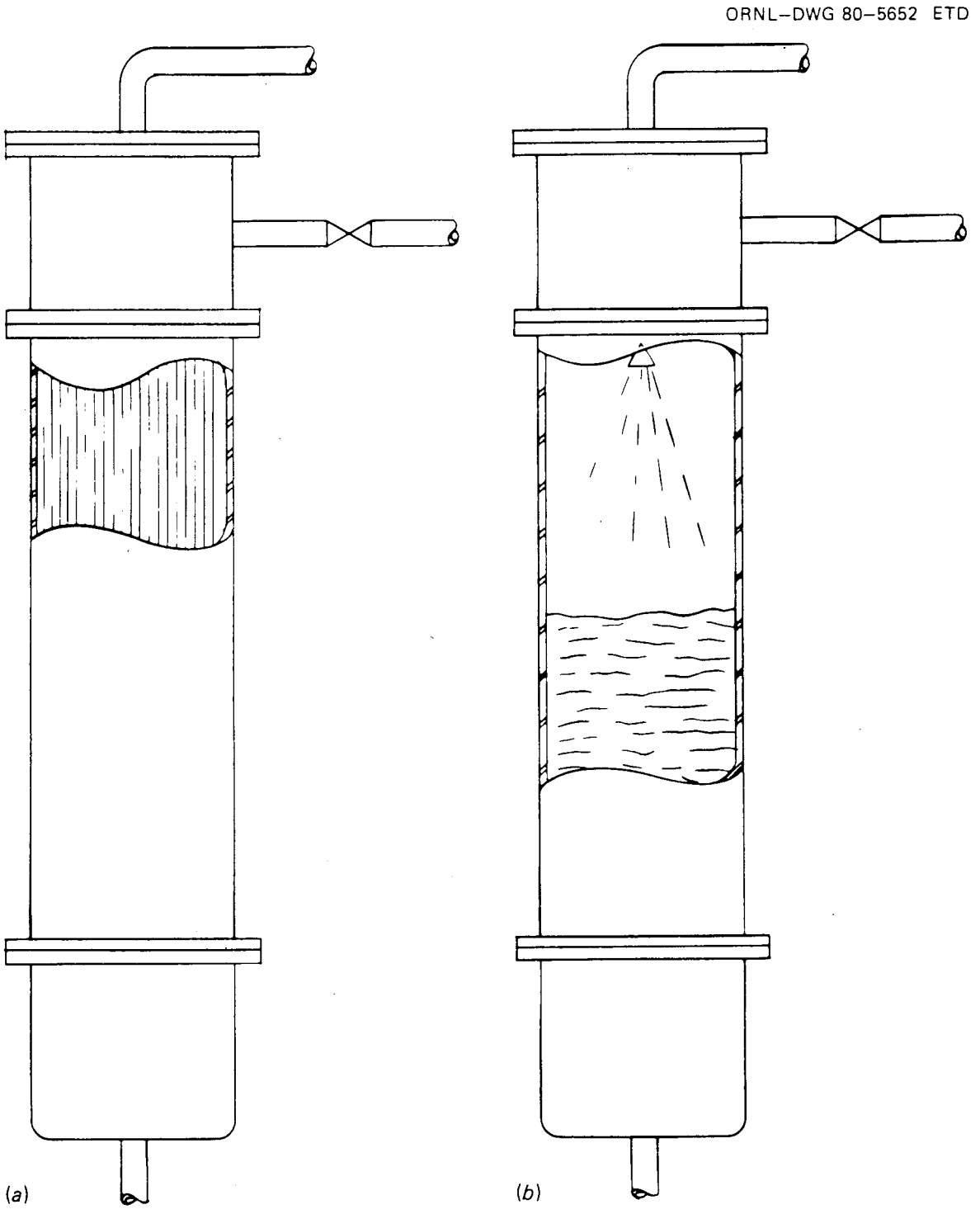

Fig. 5. Perpendicular desorber configuration.

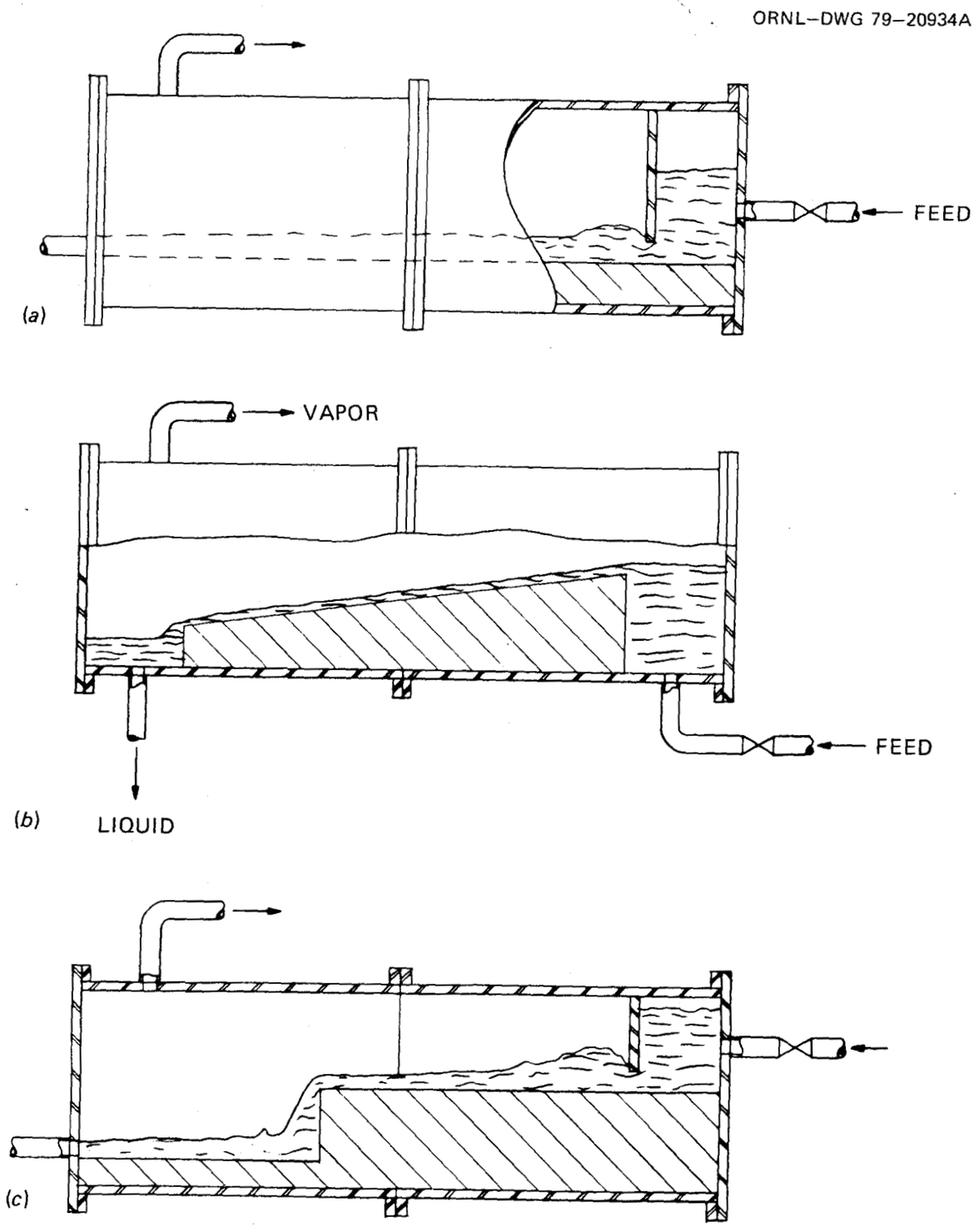

Fig. 6. Horizontal desorber configuration: (a) channel level–baffled feed; (b) channel sloped–bottom feed; (c) channel stepped–baffled feed.

to further test runs to define OTEC candidate deaerators and to obtain engineering design data.

3.3 Instrumentation

Instruments used for monitoring the desorption test loop include thermistors, well-type mercury manometers, flowmeters, and oxygen analyzers.

Water temperatures are measured at six locations by means of thermolinear probe (Yellow Spring Instrument model YSI 710X). The first point is located just before the entrance of the column. The second and third points are at 38.1-cm (15-in.) intervals deep in the packing. The fourth point is located in the water accumulator, below the packing. The fifth and sixth are positioned at the pump discharge and at the water storage tank accordingly.

The thermolinear probe network is a composite device consisting of resistors and precise thermistors that produce an output voltage linear with temperature or a resistance linear with temperature.

The temperature probe, digital ohmmeter (Data Precision Multimeter Model 3500), and associated components were selected as a system to ensure compatibility. The temperature range, accuracy, and interchangeability of the system is −1.11–37.78°C (30–100°F) ± 0.09°C. Maximum recommended time constant is 1.5 s for a probe diameter of 0.397 cm (5/32 in.) with single hex National Pipe Thread (NPT) mounting. The probe signals are processed by digital multimeter to yield the temperature, and a strip chart recorder is used to record and monitor the temperatures.

Well-type mercury manometers (Meriam, model 30EB25) measure the pressure in the gas desorption system at four locations: in the vapor line, above the distributor plate, and just above and below the packing.

The water flow rate into the desorption column is measured by two instruments, a turbine flow transducer (Flow Technology model FT-16) and a rotameter (Fischer and Porter serial No. X11-4425/2). (These two instruments are in series.) The turbine flow transducer (Flow Technology model FT-16) was installed to facilitate operation. The range of the meter is 18.93–189.3 liters/min (5.0–50 gpm), and its accuracy is ±0.05% at all

points. The flow signal is processed by flow rate monitors (Flow Technology model PRI-102D) to yield the mass flow rates.

The dissolved oxygen in the liquid is measured by oxygen analyzers at three locations: upstream of the desorption column, below the distributor plate, and downstream of the desorption column. A dissolved oxygen monitor (Beckman model 7002) is employed to measure the parts per million (ppm) of dissolved oxygen in the water. The operating ranges of the meter are 0 to 2, 0 to 10, and 0 to 20 ppm by weight of dissolved oxygen. The analyzer performs between 0 and 43.3°C (32 and 110°F), and its accuracy is ±1% of full scale at any given temperature. The polarographic oxygen sensor responds only to the partial pressure of oxygen, remaining insensitive to sample flow as long as the flow velocity is at least 45.72 cm/s (1.5 ft/s). A two-pen strip chart recorder (Brown model Y15402836) is used to record and monitor the dissolved oxygen.

In addition to the instruments listed above, a manual needle valve (Ridge Valve model B18VF8-Vec) is employed to control the vacuum pressure. Two 4000-W heaters (GE model 3A367G20) are installed in the water storage tank to replace the heat dissipated by the deaeration process. Building cooling water is used to remove the heat generated by the circulating pump. These procedures are necessary for a steady-state operating condition.

3.4 Vacuum Keeping

The existing two-stage steam-jet ejectors in the building served as the vacuum source. At an earlier stage of testing the system showed a seriously impaired performance. Its function became normal when the secondary stage nozzle and the vacuum and steam gauges were replaced by new ones. The ejector's vacuum pressure is 844 Pa (0.25 in. Hg) abs; however, better than 6.75 kPa (2 in. Hg) could not be obtained at an earlier stage of the operation. The vacuum pressure was improved to 1.69 kPa (0.5 in. Hg) by tightening the steam-line valve packing, stuffing boxes, and replacing the union at the first-stage ejector nozzle.

3.5 Air Leakage

Dry and wet vacuum tests on the loop were performed to determine the air leakage rate. Air leakage of the entire system under vacuum was improved to 1.8 g/h (0.004 lb/h) (see Appendix for calculation of air leakage rate).

This improvement was brought about by tightening all joints and covering them with the sealant Apiezon so that while the system is under vacuum, Apiezon is drawn into crevices.

4. ANALYSIS

4.1 Basic Design of Vacuum Desorber

When starting to design a vacuum degasser, one must have all data on

1. the liquid [e.g., for water (sea water inclusive): flow, temperature, and density];
2. type and quantity of gases in solution in ppm in the liquid phase under standard conditions (at the inlet to the vacuum desorber) (when surface or sea water is used without any chemical treatment, the solubility values of O_2 and N_2 for the given temperature will be chosen);
3. the imposed outlet concentration in ppm of the undesirable gas or gases;
4. some other helpful information such as local conditions — available height (mostly for off-shore platforms) and local economic conditions (if some chemical treatment is involved, such as acid for bicarbonate reduction, possible chemical reactions and the resulting influences on gas volumes must be established).

4.2 Principles of Vacuum Degasification in a Packed Column

The transfer of mass (air from water) in a packed column takes place throughout the column at the interface between the liquid and gas. Both liquid and gas are moving countercurrently, with the liquid making its way through the maze of passages in and around the packing to the bottom of the column and air rising through the same passages to the top of the column.

When the temperature and vacuum pressure of the test media remain constant, then the equilibrium concentration of solute gas is constant. The concentration of the liquid in the test section decreases continuously as the liquid flows through the test section.

The equilibrium concentration of solute gas and the concentration of liquid in the test section are plotted against the height of the column in Fig. 7. The horizontal line represents the equilibrium concentration of

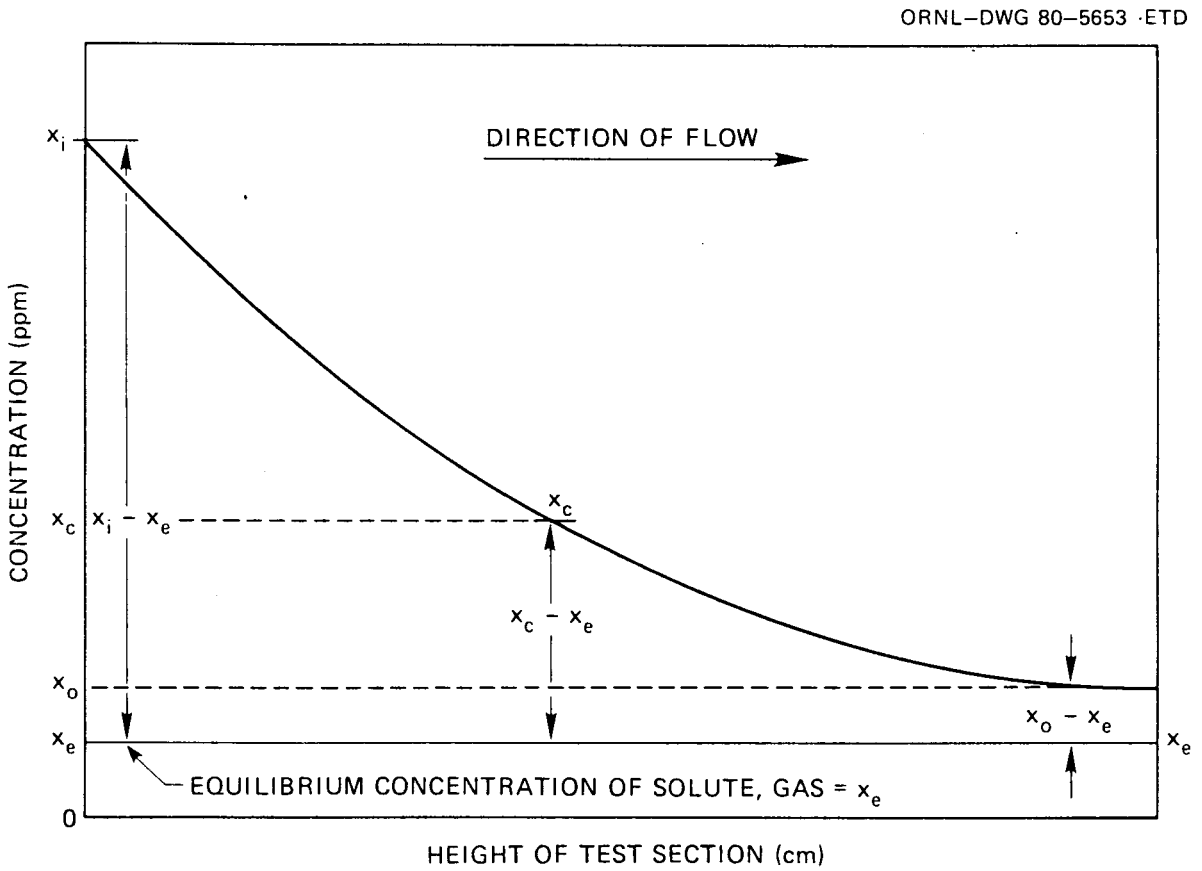

Fig. 7. Concentration-height of test section.

solute gas, and the curved line above it is the declining concentration of the liquid in the test section. In Fig. 7, the inlet and outlet liquid concentrations are x_i and x_o, respectively, and the constant equilibrium concentration of solute is x_e. At a length L from the entrance end of the test section, the liquid concentration is x_c, and the local difference between the equilibrium concentration and liquid is $(x_c - x_e)$. This concentration difference is called a point concentration difference. At the inlet of the test section, the point concentration difference is $(x_i - x_e)$; and at the exit end, it is $(x_o - x_e)$.

In the vacuum desorption unit, no gas is fed into the tower. The partial pressure of the undesirable gas is decreased by the vacuum created in the desorption unit. The gas phase consists of a mixture of gases (undesirable and others) plus the vapor.

In both operations, decreasing the partial pressure of the undesirable gas in contact with the liquid phase causes an increase in the mass transfer capacity of the gas to be eliminated and thus accelerates its passage from the liquid to the gas phase.

The transfer between phases is carried out across the interface; thus, the larger the surface of the interface, the higher the efficiency of the unit. The vacuum desorber is a hermetically closed tower. It may be filled with solid packed material or contain a number of plates, it may be an empty tower into which the liquid under treatment is sprayed, or it may be a combination of the above systems.

The choice among the different types of vacuum desorption depends, among other factors, on (1) the type of liquid to be treated (e.g. viscosity), (2) the grade of desorption to be obtained, and (3) the relative cost.

If the liquid to be treated is water (including sea water) and if the concentration of the remaining (undesirable) gas has to be very low (sometimes 10 to 15 ppb only), the packed tower combined with a top spray arrangement on the incoming water line is an attractive solution.

The calculations criteria for a vacuum desorber are based on the assumption that

1. the liquid to be treated is water,
2. the soluble gases (air) to be eliminated are not reacting chemically with the water,
3. the laws of perfect gases are applicable,
4. the temperature in the tower is constant and equal to the temperature of the water,
5. the vacuum desorber is a packed tower (Raschig, Pall rings).

The theories and laws that govern the practical design criteria of deaeration equipment include the ideal gas law, Henry's law of gas dissolution, and Dalton's law of partial pressure. Thus,

$$pV = nRT \ , \qquad (4.1)$$

and for continuous flow, by replacing V by QG and n = m/M with

$$m = 10^{-3}\ Q_L(C - C')\ , \tag{4.2}$$

we obtain

$$Q_G = \frac{10^{-3}\ Q_L(C - C')}{PM}\ RT\ . \tag{4.3}$$

4.2.1 Solubility of gases in a liquid (Henry's law)

Henry's law is applicable to solutions in equilibrium, with relatively low concentrations and low total pressure. At a constant temperature, the partial pressure of a constituent of a gas mixture in contact with a liquid phase is proportional to the concentration of that constituent in the liquid phase. Thus the solubility of a gas in a liquid is proportional to its partial pressure in the gas phase. In a given temperature, the molar fraction of a gas is divided between the liquid and gas phases according to a constant ratio H known as Henry's constant:

$$H = (p/pa)(1/x)\ , \tag{4.4}$$

where x is the mole fraction of the gas in the liquid phase. The mole fraction is the ratio of the number of moles contained in a given weight of the solution to the total moles of all constituents. Thus

$$x = \frac{n}{n + n_L}\ ; \tag{4.5}$$

n is very small if compared with n_L. We admit that

$$n + n_L = n_L \tag{4.6}$$

(symbol L for liquid); thus

$$n = \frac{m}{M} \text{ and } n_L = \frac{m_L}{M_L}\ . \tag{4.7}$$

By replacing Eqs. (4.5), (4.6), and (4.7) in Eq. (4.4) we obtain

$$H = \frac{p \cdot m_L \cdot M}{pa \cdot m \cdot M_L} , \tag{4.8}$$

where

$$m_L = Q_L \rho_L \text{ and } m = 10^{-3} Q_L C' . \tag{4.9}$$

Henry's law applies to a solution in equilibrium. In a vacuum desorption featuring continuous operation, we have to maintain an interface concentration (C_i) lower than (C') and a gas pressure (p) lower than (p_i) to reach the desired concentration (C') in the liquid-phase. Thus

$$m = 10^{-3} Q_L C_i , \tag{4.10}$$

and by replacing Eqs. (4.9) and (4.10) in Eq. (4.8) we obtain

$$C_i = \frac{p}{pa} \cdot \frac{10^3 \rho}{H} \cdot \frac{M}{M_L} . \tag{4.11}$$

4.2.2 Dalton's law

The pressure of a mixture of gases is the sum of the pressures that each of the gases would exert if it alone were present in the containing vessel. Therefore,

$$p = p_L + p_r + p_x + p_y \cdots , \tag{4.12}$$

where p is total pressure in the vessel and p_L, p_r, p_x, and p_y are, respectively partial pressures of liquid vapor, reference gas (gas to be eliminated), x, y, and other gases.

4.3 Mass Transfer Fundamentals

The packed column is useful in carrying out mass transfer between gas and liquid when the two fluids pass countercurrent to each other. A packed column is used in the first part of this investigation to verify the test loop performance. The relation between the gas and liquid film

resistances and the total resistance to mass transfer is expressed as follows:

$$\frac{1}{K_G a} = \frac{1}{k_G a} + \frac{1}{Hk_L a} = \frac{1}{HK_L a} \ . \tag{4.13}$$

4.4 Development of Transfer Unit

Chilton and Colburn[18] advanced an alternative concept of a transfer unit that is useful for interpreting and correlating mass-transfer data. It is based on the idea of dividing the mass transfer medium (packed section) into two parts. The first part is a dimensionless function of concentrations and concentration driving force only, called the number of transfer units (NTU). The second part, the depth of transfer media (packing) required by a single transfer unit, is called the height of one transfer unit (HTU). The total height of transfer media (packed) section is

$$h = (NTU)(HTU) \ . \tag{4.14}$$

The HTU is closely related to the mass transfer coefficient, and the two quantities are essentially equivalent. However, the HTU is simpler to visualize, because its dimension is simply length and it is measured in meters (feet). The usual order of magnitude of this quantity is 0.15 to 1.52 m (0.5 to 5 ft). The units of the mass-transfer coefficient are more complex, and numerical magnitudes vary widely.

In mass transfer the driving force is the numerical value of NTU. The total depth of packing, of course, is the same; thus, by Eq. (4.14), the product of NTU and HTU is always constant.

The definition of transfer unit is completed by adopting the following general equation for vacuum deaeration:

$$-NTU = \int_{x_i}^{x_o} \frac{dx}{x - x_e} = \ln \frac{x_o - x_e}{x_i - x_e} \ , \tag{4.15}$$

or

$$NTU = \ln \frac{x_i - x_e}{x_o - x_e} . \tag{4.16}$$

In a vacuum column deaerator, the HTU and NTU are related as follows:

$$\frac{1}{HTU} = \frac{d(NTU)}{d(h)} = \frac{\ln [(x_i - x_e)/(x_o - x_e)]}{(h + h_{end})} , \tag{4.17}$$

where h is the actual height of the packing and h_{end} is the end effect, that is, the additional packing height that would produce the mass transfer which occurs in the inlet distributor and in all other parts of the column except the packing.

5. RESULTS OF INITIAL TESTS

The first series of runs, 110 in all, was completed. Liquid samples taken from the top of the packing were analyzed by the Winkler titration method to determine the concentration in parts per million of oxygen; an oxygen analyzer was used to determine the oxygen concentration leaving the desorption column. Raschig-ring packing of 3.81 cm (1-1/2 in.) was used. The effective packing height was varied from 25.4 to 81.28 cm (10 to 32 in.) by operating the system at different liquid levels in the packing. Liquid flow rates and vacuum pressures varied from 26×10^3 to 134×10^3 kg/(m^{2}h) [5,350 to 27,400 lb/(h·ft^2)] and from 7.36 to 34 kPa (2.18 to 10.07 in. Hg abs) respectively.

The NTU values were plotted against packing height, as in Fig. 8, for each group of runs for which all other operating variables were constant. From Eq. (4.16), the natural logarithm of each slope is the NTU for the corresponding operating conditions. These were found to fall on straight lines, indicating uniform liquid distribution and liquid-gas interfacial area. From Eq. (4.17), the slope of each of these lines is the reciprocal of the HTU of the packing alone for the corresponding operating conditions.

Extrapolating the lines of Fig. 8 to zero NTU gives the height of additional packing that would be equivalent to the end effect. In the first series of tests the end effects were localized above the packing to the drip below the distribution plate and the liquid line leading to the desorption column. The end effect will be minimized by placing a partition in the upper portion of the test section and by improving the distributor system so that water comes down through ten 15-cm-long tubes and actually touches the top of the packing. In this case, the liquid flows down without falling through the air at all and spreads out with no splashing.

As seen in Fig. 9, the HTU increased with the water flow rate. Sherwood and Holloway[4] investigated liquid film resistance in the desorption of oxygen, hydrogen, and carbon dioxide from water by a stream of air. For 1.5-in. Raschig rings, straight line M in Fig. 9 represents the results. In the first series of tests the HTU of the present study,

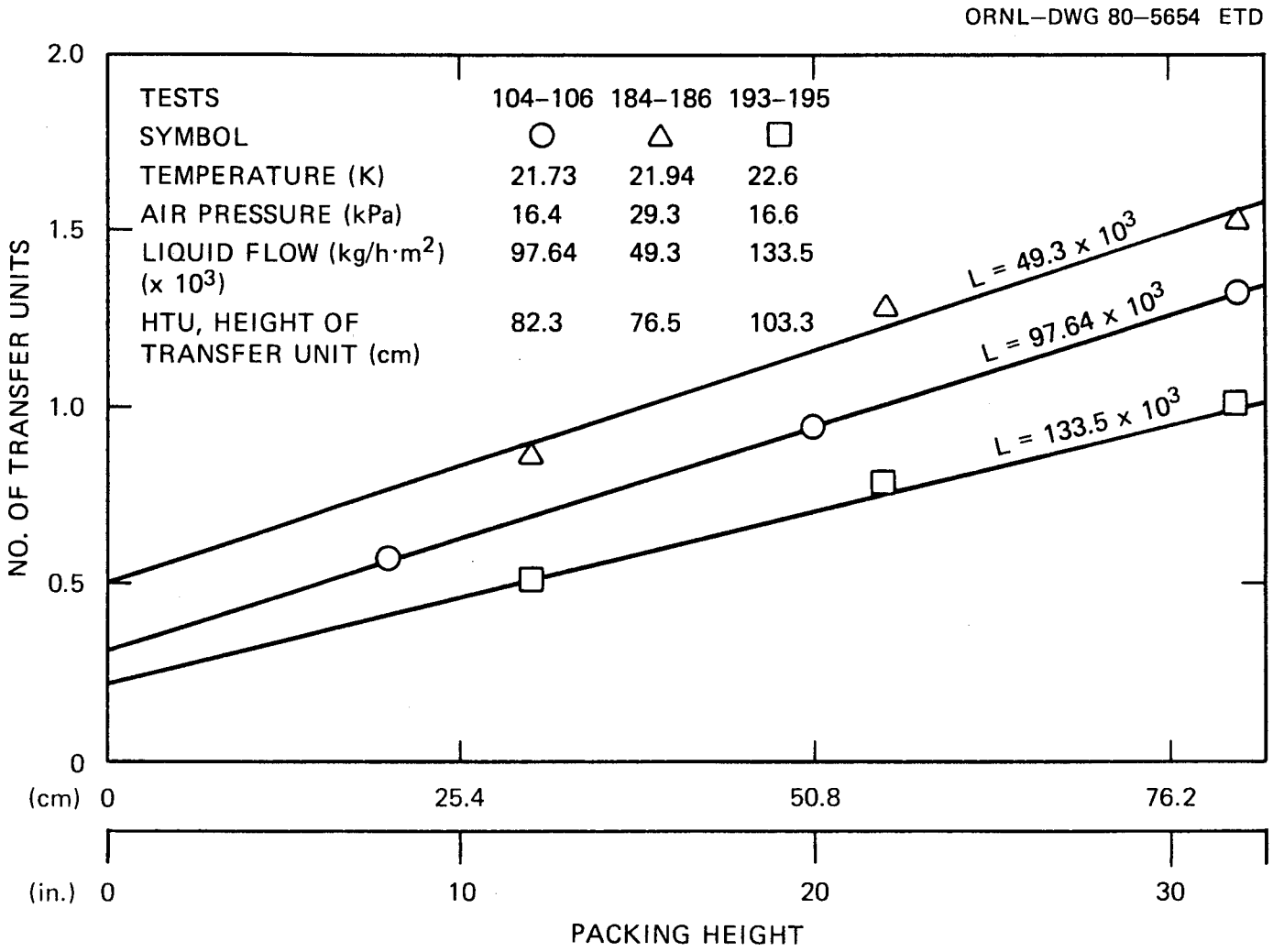

Fig. 8. Relationship between number of transfer units and packing height at different liquid flow rates.

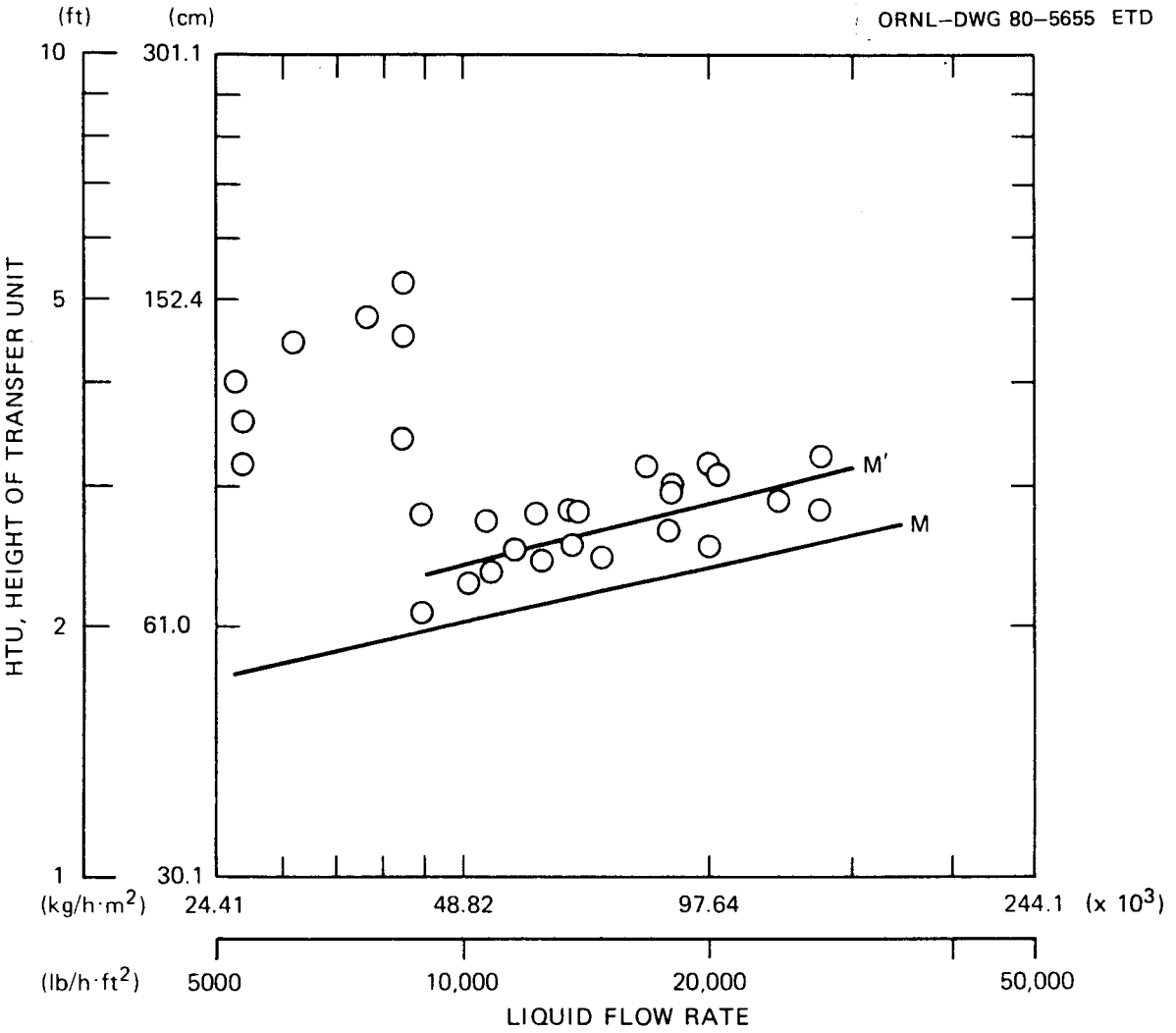

Fig. 9. Comparison of test data with results of Sherwood and Holloway.

straight line M′, is somewhat higher than the HTU of Sherwood and Holloway's work. The difference between curves M and M′ may be caused by the end effect and the nature of vacuum deaeration. Previous investigators have not discussed the effect of the vacuum pressure in a packed-column deaeration study.

At low water flow rate [i.e., below 41.5×10^3 kg/(h·m^2)], the computed HTU results deviate from the line M′, as can be seen in Fig. 9. Uneven flow distribution, together with the eccentric end effect at vacuum condition, is suspected as the cause of the increase in HTU values.

Data obtained in the first series are presented in Tables 2 and 3.

Table 2. Data of first series oxygen desorption in column packed with 3.81-cm (1.5-in.) Raschig ring

Because of end effects the data of this series should not be used directly for design purposes.

Test series	Packing height (cm)	Inlet x_i (ppm)	Outlet x_o (ppm)	Equilibrium x_e (ppm)	Packing NTU	Temperature (°C)
101	25.4	4.45	3.1	1.42	0.65	21.8
102	53.34	4.40	2.6	1.42	1.05	21.8
103	81.28	4.63	2.4	1.42	1.36	21.8
104	20.32	4.97	3.45	1.44	0.57	21.73
105	55.9	4.97	2.85	1.44	0.94	21.73
106	81.28	4.63	2.45	1.44	1.32	21.73
107	0	5.06	4.05	1.66	0.352	21.92
108	20.32	4.88	3.45	1.66	0.587	21.92
109	50.8	4.85	2.75	1.66	1.074	21.92
110	81.28	4.74	2.35	1.66	1.496	21.92
111	0	5.37	4.15	1.43	0.371	21.83
112	20.32	5.12	3.55	1.43	0.554	21.83
113	50.8	4.90	2.95	1.43	0.825	21.83
114	81.28	4.83	2.50	1.43	1.156	21.83
115	0	4.08	3.75	0.634	0.1	22.89
116	20.32	3.75	2.95	0.634	0.297	22.89
117	50.8	3.61	2.30	0.634	0.58	22.89
118	81.28	3.61	1.80	0.634	0.94	22.89
119	0	3.66	3.4	0.627	0.09	23.1
120	20.32	3.52	2.7	0.627	0.33	23.1
121	50.8		2.0	0.635		23.1
122	81.28	3.30	1.60	0.635	1.02	23.1
123	0	4.97	4.58	1.03	0.104	21.44
124	17.78	4.92	3.95	1.03	0.287	21.44
125	50.8	4.60	3.00	1.03	0.595	21.44
126	81.28	4.60	2.50	1.03	0.887	21.44
127	0		4.51	0.769		21.76
128	17.78	4.01	3.30	0.769	0.247	21.76
129	50.8	3.81	2.55	0.769	0.535	21.76
130	81.28	3.84	2.37	0.769	0.651	21.76
131	0	6.32	5.35	2.952	0.340	22.4
132	20.32	6.16	4.80	2.952	0.552	22.4
133	50.8	6.00	4.30	2.952	0.816	22.4
134	81.28	5.80	3.85	2.952	1.154	22.4
135	0	6.33	4.60	2.851	0.688	21.8
136	20.32	6.39	4.23	2.851	0.942	21.8
137	50.8	6.14	3.80	2.851	1.243	21.8
138	81.28	6.05	3.55	2.851	1.521	21.8
139	0	6.25	5.1	2.615	0.38	22.3
140	20.32	6.07	4.85	2.615	0.436	22.3
141	50.8	5.64	3.85	2.615	0.896	22.3
142	81.28	5.73	3.75	2.615	1.01	22.3
143	0	6.03	4.3	2.7	0.733	21.82
144	20.32	5.76	4.05	2.7	0.82	21.82
145	50.8	6.09	3.75	2.7	1.17	21.82
146	81.28	6.12	3.35	2.7	1.67	21.82
147	0	6.19	4.55	2.65	0.622	21.73
148	20.32	6.14	4.10	2.65	0.878	21.73
149	50.8	5.82	3.70	2.65	1.105	21.73
150	81.28	5.85	3.35	2.65	1.52	21.73
151	30.48	5.36	3.75	1.9	0.626	21.83
152	55.9	5.27	3.40	1.9	0.809	21.83
153	81.28	5.19	3.10	1.9	1.009	21.83

Table 2 (continued)

Test series	Packing height (cm)	Inlet x_i (ppm)	Outlet x_o (ppm)	Equilibrium x_e (ppm)	Packing NTU	Temperature (°C)
154	30.48	5.11	3.35	1.85	0.776	22.4
155	55.9	5.10	3.05	1.85	0.996	22.4
156	81.28	4.91	2.90	1.85	1.07	22.4
157	30.48	5.01	3.37	1.85	0.732	22.25
158	55.9	4.97	3.0	1.85	0.998	22.25
159	81.28	4.99	2.65	1.85	1.367	22.25
160	30.48	5.1	3.5	1.95	0.709	22.2
161	55.9	5.27	3.05	1.95	1.105	22.2
162	81.28	5.25	2.8	1.95	1.356	22.2
163	30.48	4.82	3.5	1.58	0.524	23.3
164	55.9	4.59	3.1	1.58	0.685	23.3
165	81.28	4.40	2.75	1.58	0.882	23.3
166	30.48	4.79	3.4	1.57	0.55	23.0
167	55.9	4.76	2.95	1.57	0.84	23.0
168	81.28	4.63	2.45	1.57	1.24	23.0
169	30.48	5.01	3.35	1.81	0.73	23.0
170	55.9	4.94	2.90	1.81	1.06	23.0
171	81.28	4.91	2.45	1.81	1.58	23.0
172	30.48	4.92	3.45	1.8	0.636	22.92
173	55.9	5.08	3.00	1.8	1.003	22.92
174	81.28	4.8	2.72	1.8	1.18	22.92
175	30.48	6.27	3.8	2.645	1.144	21.94
176	55.9	5.91	3.45	2.645	1.40	21.94
177	81.28	5.97	3.25	2.645	1.704	21.94
178	30.48	5.28	3.5	1.64	0.671	21.9
179	55.9	5.07	3.0	1.64	0.925	21.9
180	81.28	5.10	2.65	1.64	1.231	21.9
181	30.48	4.83	3.25	1.72	0.709	22.03
182	55.9	4.76	2.91	1.72	0.937	22.03
183	81.28	4.72	2.55	1.72	1.283	22.03
184	30.48	5.62	3.85	2.57	0.868	21.94
185	55.9	5.60	3.41	2.57	1.283	21.94
186	81.28	5.73	3.25	2.57	1.536	21.94
187	30.48	5.73	3.55	2.43	1.081	22.92
188	55.9	5.29	3.35	2.43	1.134	22.92
189	81.28	5.71	2.95	2.43	1.84	22.92
190	30.48	4.83	2.9	1.425	0.837	22.92
191	55.9	4.23	2.39	1.425	1.007	22.92
192	81.28	4.51	2.17	1.425	1.421	22.92
193	30.48	4.85	3.42	1.27	0.51	22.6
194	55.9	5.05	3.00	1.27	0.782	22.6
195	81.28	4.76	2.55	1.27	1.003	22.6
196	30.48	5.71	3.75	2.48	0.933	22.6
197	55.9	5.80	3.55	2.48	1.132	22.6
198	81.28	5.71	3.20	2.48	1.5	21.2
199	30.48	5.58	3.63	1.98	0.781	21.2
200	55.9	5.71	3.25	1.98	1.08	21.2
201	81.28	5.40	2.95	1.98	1.26	21.2
202	30.48	5.65	3.85	2.4	0.81	21.2
203	55.9	5.94	3.60	2.4	1.08	21.2
204	81.28	6.91	3.25	2.4	1.42	21.2
205	30.48	5.68	3.55	2.17	0.933	19.5
206	55.9	5.87	3.42	2.17	1.08	19.5
207	81.28	5.44	3.10	2.17	1.26	19.5
208	30.48	6.12	3.91	2.46	0.928	20.11
209	55.9	4.87	3.66	2.46	1.099	20.11
210	81.28	5.76	3.30	2.46	1.37	20.11

Table 3. Data of first series oxygen desorption in column packed with 3.81-cm (1.5-in.) Raschig ring

Test series	$L \times 10^3$ [kg/(h·m^2)]	Pair (kPa)	Temperature (°C)	Packing HTU (cm)	HTU by use of empirical values[a]
101–103	61.6	16.2	21.8	79.25	64.6
104–106	97.64	16.4	21.73	82.3	71.63
107–110	66.8	18.98	21.92	69.8	65.84
111–114	97.64	16.3	21.83	104.8	71.63
115–118	97.8	7.4	22.89	97.5	69.8
119–122	61.75	7.4	23.1	87.8	62.5
123–126	82.3	11.6	21.44	104.5	69.5
127–130	37.4	8.75	21.76	160.0	57.9
130–134	26.1	34.0	22.40	101.5	52.7
135–138	88.3	32.8	21.8	98.75	61.3
139–142	26.3	30.0	22.3	115.8	54.2
143–146	87.6	30.7	21.82	86.26	70.1
147–150	117.3	30.2	21.73	94.2	74.98
151–153	25.7	21.7	21.83	131.1	53.34
154–156	41.4	21.3	22.4	171.3	58.5
157–159	56.8	21.2	22.25	80.5	62.8
160–162	72.05	22.3	22.2	78.94	66.14
163–165	30.5	18.6	23.3	141.7	53.6
166–168	50.4	18.3	23.0	73.1	60.0
169–171	66.7	21.14	23.0	59.74	64.0
172–174	87.0	20.9	22.92	93.3	68.0
175–177	67.1	30.2	21.94	90.8	65.53
178–180	65.8	18.7	21.90	90.83	65.5
181–183	49.2	19.65	22.03	88.4	60.96
184–186	49.3	29.3	21.94	76.5	60.96
187–189	43.7	28.3	22.92	67.1	58.52
190–192	43.7	16.6	22.92	87.2	58.52
193–195	133.5	16.6	22.6	103.3	75.3
196–198	133.8	28.7	22.6	89.92	75.3
198–201	66.1	22.3	21.2	105.5	66.75
202–204	65.9	27.0	21.2	83.82	66.75
205–207	41.2	23.6	19.5	156.4	62.5
208–210	41.2	27.1	20.11	115.2	61.3

[a]T. K. Sherwood and A. L. Holloway, "Performance of Packed Towers — Liquid Film Data for Several Packing," *Trans. AICHE* 36, 39 (1940).

6. PROBLEMS AND UNCERTAINTIES

The HTU and NTU are related according to Eq. (4.14), and the NTU is determined as follows:

$$NTU = \ln [(x_i - x_e)/(x_o - x_e)] ,$$

where x_i and x_o are ppm of oxygen entering and leaving the test column respectively, and x_e is the ppm of oxygen at the equilibrium test condition. Correct measurement of x_i and x_o is important in the analysis.

The data available from these limited verification experiments indicate an HTU value higher than that obtained by Sherwood and Holloway.[13] This discrepancy could originate either in the operating conditions of the ORNL tests or in the performance of the measuring instrumentation.

6.1 Operational Factors

The operational factors that could cause the discrepancy are as follows.

1. Verification runs indicate that the system performs better in a moderate vacuum than in a high vacuum pressure, partly because a portion of deareation takes place in the line leading to the desorption column.

2. The ORNL data were obtained at a liquid flow rate of 111×10^3 kg/(h·m^2) [22,750 lb/(h·ft^2)] or 1.9 liters/s (30 gpm) in the test section; this is higher than the loading limit of 97.6×10^3 kg/(h·m^2) [20,000 lb/(h·ft^2)] recommended by previous investigators.

3. Another area of concern in the closed test loop is the air absorber. The degassed water from the test section is reaerated by injecting compressed air into the returned water in the water storage tank. The average residence time of water in the absorber is ~5 min. This aeration system could bring in the dissolved oxygen at as much as 70–80% of its saturation value. Although the results of the vacuum deaeration tests should not, in theory, be affected by the percentage of air saturation of the feed water, in practice, this saturation does impose a higher-order sensitivity requirement on the data acquisition procedure.

6.2 Measurement Factors

The performance of the oxygen analyzer sensor in the vacuum environment of these experiments is subject to question. The impact of this uncertainty in oxygen concentration measurement is apparent from Eq. (4.17), relating HTU to oxygen concentration. The sensor is composed of a gold cathode and a silver anode, electrically connected by potassium chloride electrolyte. A constant electrical potential thus is present across the two electrodes.

A gas-permeable Teflon membrane, fitted firmly against the gold cathode, separates the electrodes from the process stream. Oxygen from the sample diffuses through the membrane and is reduced at the gold cathode. The resultant electrical current flow between anode and cathode is proportional to the partial pressure of oxygen in the sample. The sensor was installed in a portion of the loop where it was exposed to pressures as low as 1.4 kPa (—14.5 psig). Under these conditions, the Teflon membrane may fit loosely against the gold cathode, causing inaccurate reading of ppm of oxygen. The vendor advised that a pin hole in the pressure-compensating diaphragm in the fill port of the oxygen sensor could eliminate this problem. However, very little improvement was observed after the pin-hole modification.

Additional tests have shown that (1) when deaeration takes place in a low vacuum environment, the flow rate through the oxygen sensor drops below the minimum flow requirement, with a result of inaccurate readings of the concentration of dissolved oxygen, and (2) the sensor is insensitive to sample flow rate as long as the flow rate passing the sensor chamber is at least 95 ml/s (1.5 gpm).

To alleviate this problem of uncertainty in the sensor readings of dissolved oxygen under vacuum conditions, the sensor chambers have been moved to a test loop location where they will be exposed to positive pressure and be guaranteed minimum water flow rate through their flow chambers.

7. CONCLUSIONS

The following conclusions may be drawn from the experimental data of the OTEC gas desorption study.

1. In this study, the HTU was found to be somewhat greater than that reported by earlier investigators Sherwood and Holloway. Thus, from the present experiment, at 25°C the HTU for air desorption from water on 1.5-in. Raschig rings can be expressed as a function of water flow rate L by

$$HTU = 4.93\ L^{0.25}\ ; \tag{7.1}$$

this is shown as line M′ in Fig. 9. In contrast, the Sherwood and Holloway results (line M, Fig. 9) for oxygen, hydrogen, and carbon dioxide desorption from water at 25°C on 1.5-in. Raschig rings is described by

$$HTU = 5.38\ L^{0.22}\ . \tag{7.2}$$

The observed discrepancy may be due to differences in end effects and in vacuum versus atmospheric pressure operation.

2. At a low water flow rate, below 41.5×10^3 kg/(h·m^2), the HTU results deviate from the line M′ (Fig. 9). Uneven flow distribution, accompanied by the eccentric end effect at vacuum condition, is the suspected cause of the high experimental HTU values.

3. The HTU appears to be independent of vacuum pressure. The values of HTU, plotted in Fig. 10 as a function of pressure, scatter between 60 to 105 cm (2.0 to 3.5 ft) at any vacuum pressure. Most of the data (Table 3) were obtained at temperatures within a few degrees of 25°C, and the values used in Fig. 10 have been corrected to 25°C by empirical relations.

4. The end effect depends considerably on vacuum pressure and slightly on flow rate or temperature.

The data in Fig. 11 relate the deaerator vacuum pressure to the corresponding end effect; air pressure and end effect are correlated as

$$P_{air} = 3.35(h_{end})^{0.53}\ .$$

ORNL-DWG 80-5656 ETD

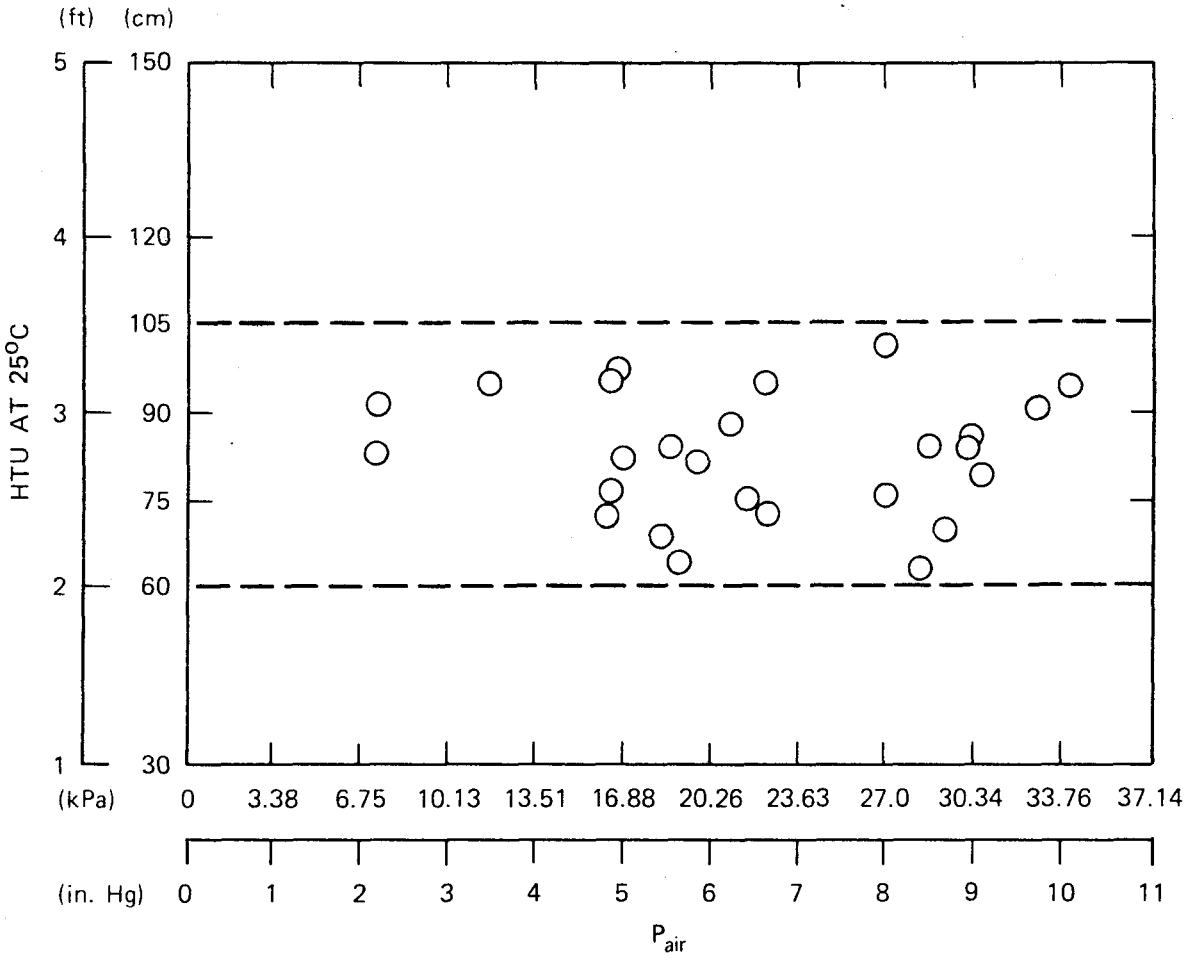

Fig. 10. Effect of vacuum pressure on height of transfer unit at constant temperature.

The end effect h_{end} is the additional mass transfer that occurs in the inlet distributor and in all other parts except the packing. The major portion of the end effect takes place in the water line leading to the desorption column. The end effect could be represented by the number of transfer units NTU_o. The relation between air pressure (vacuum) and NTU_o, shown in Fig. 12, is expressed by

$$P_{air} = 36.97\ (NTU_o)^{0.624}\ .$$

ORNL-DWG 80-5657 ETD

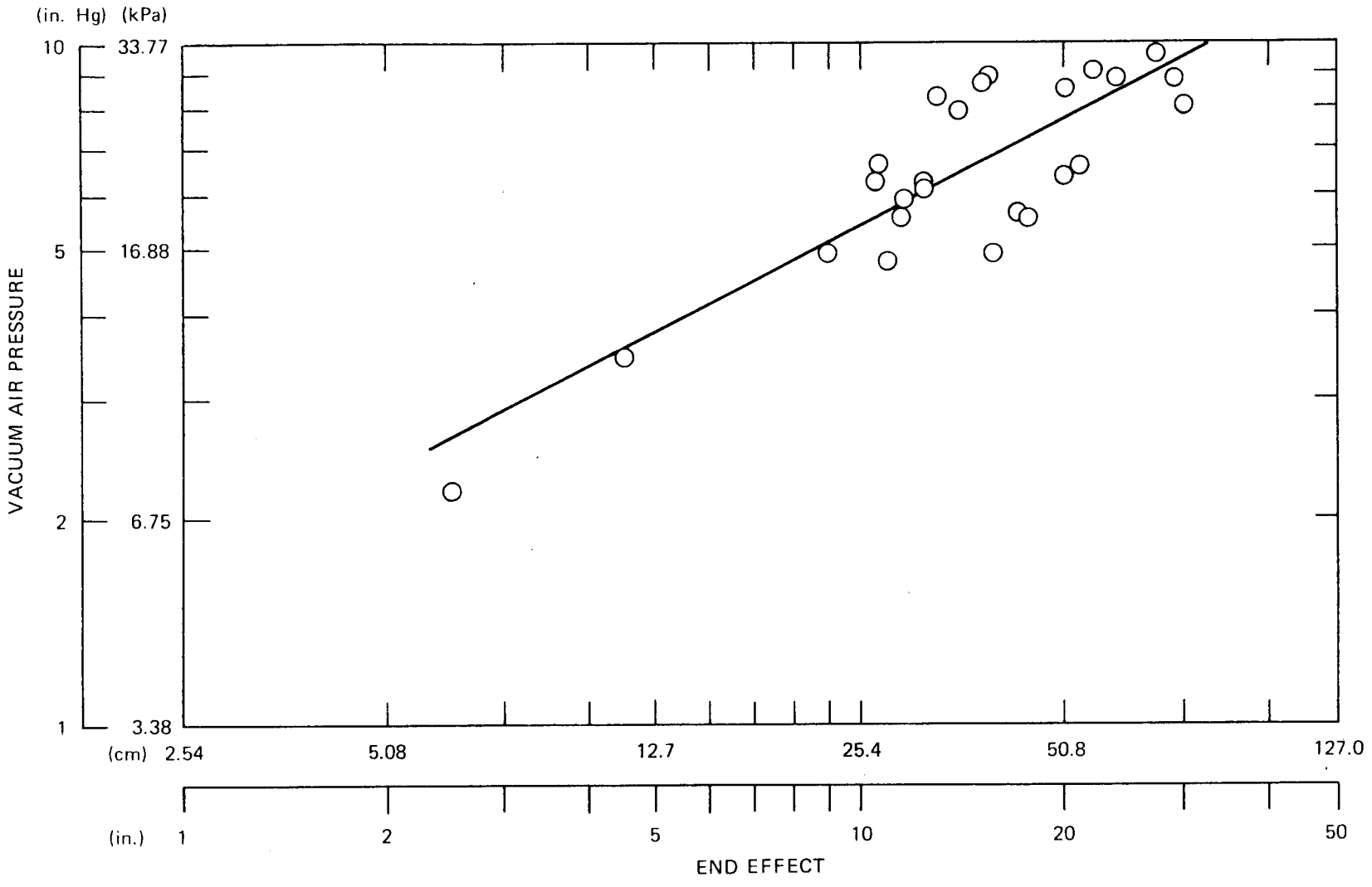

Fig. 11. Variation of end effect (in.) with respect to vacuum pressure.

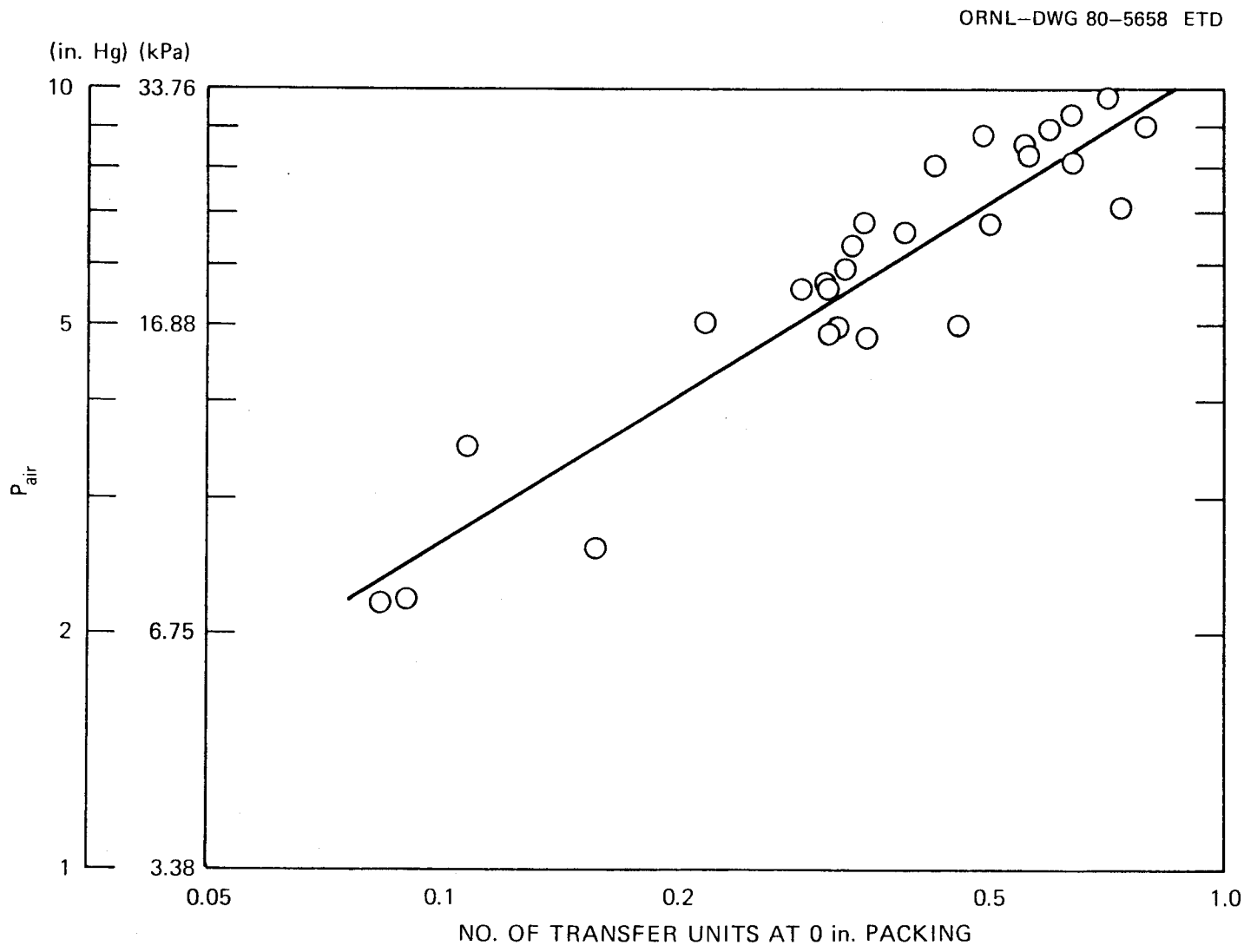

Fig. 12. Relation of vacuum air pressure and NTU.

8. NOMENCLATURE

a = effective area of liquid gas interface per unit volume m^2/m^3

$(C - C')$ = concentration of gas to be eliminated in the liquid phase, mg/liter

D = coefficient of diffusion — solute gas in liquid, m^2/h

G = inert gas flow rate, $\frac{kg}{(h)(m^2)}$

h = height of packing, cm

h_{end} = height of packing equivalent to end effects, cm

H = Henry's law constant, $\frac{(kmol/m^3)}{kPa}$

HTU = height of transfer unit, using liquid, cm

K_Ga = overall coefficient based on partial pressure, $\frac{kmol}{(h)(m^3)(kPa)}$

k_Ga = gas film coefficient, $\frac{kmol}{(h)(m^3)(kPa)}$

K_La = overall coefficient based on concentration, $\frac{kmol}{(h)(m^3)[kg\cdot(mole/m^3)]}$

k_La = liquid film coefficient, $\frac{kmol}{(h)(m^3)[kg\cdot(mole/m^3)]}$

L = liquid flow rate, $kg/(h\cdot m^2)$

M = mass of gas, g·mole

m = gas mass flow rate, kg/h

m_L = liquid mass flow rate, kg/h

NTU = number of transfer units

NTU_o = number of transfer units corresponding to end effect

n = number of moles to be transfered in unit time, kmol/h

p = pressure of gas in the gas phase, kPa

p_a = atmospheric pressure, Pa = 100 kPa at sea level

p_{air} = absolute vacuum air pressure, kPa

Q_G, Q_L = gas and liquid flow rate, respectively, m^3/h

r = empirical constant

R = gas constant, $(kPa\cdot m^3)/(°K\cdot kmol)$

s = empirical constant

x_L = concentration of solute in liquid entering tower, $\frac{\text{kg gas}}{\text{kg water}}$ (10^6) (ppm)

x_o = concentration of solute in liquid leaving tower, $\frac{\text{kg gas}}{\text{kg water}}$ (10^6) (ppm)

x_e = concentration of solute in liquid in equilbrium with gas phase

y = empirical constant

z = empirical constant

α = empirical constant

β = empirical constant

μ = viscosity, Pa•s

ρ = density, kg/m^3

REFERENCES

1. T. C. G. Carlson and W. P. Gross, "OTEC — A Comprehensive Energy Analysis," *Mech. Eng.*, pp. 32—39 (January 1980).

2. A. D. Watt, F. S. Mathews, and R. E. Hathaway, *Open Cycle Thermal Energy Conversion — A Preliminary Engineering Evaluation*, ALO/3723-76/3 (July 1977).

3. Westinghouse Electric Corp., *100 MWe OTEC Alternate Power Systems*, Final Report, DOE Contract EG-77-C-05-1473 (March 1979).

4. C. Zener et al., "Recent Developments in the Foam OTEC System," p. 9.2-1 in *Proceedings of the Sixth Annual OTEC Conference, Washington, D.C., June 19—22, 1979,* Vol. 1, CONF-79631.

5. S. L. Ridgway et al., *Mist Flow Ocean Thermal Energy Process*, Final Report, ORO-1684 (September 1978).

6. R. E. Emmert and R. L. Pigford, "A Study of Gas Absorption in Falling Liquid Films," *Chem. Eng. Prog.* 50, 2 (1954).

7. S. Lynn et al., "Absorption Studies in the Light of the Penetration Theory," I. Long Wetted-Wall Columns," *Chem. Eng. Sci.* 4, 2 (April 1955).

8. A. P. Lamourella and O. C. Sandall, "Gas Absorption into a Turbulent Liquid," *Chem. Eng. Sci.* 27 (1972).

9. J. T. Lewis and W. G. Whitman, "Principles of Gas Absorption," p. 1215 in *Industrial and Engineering Chemistry*, vol. XVI (1924).

10. R. Higbie, "The Rate of Absorption of a Pure Gas into a Liquid During Short Period of Exposure," *Trans. Am. Inst. Chem. Eng.* 3, 365 (1935).

11. P. V. Danckwerts, "Significance of Liquid-Film Coefficients in Gas Absorption," *Ind. Eng. Chem.* 43, 1460 (1951).

12. V. G. Levich, Physicochemical Hydrodynamics, Prentice-Hall, New York, 1962.

13. T. K. Sherwood and A. L. Holloway, "Performance of Packed Towers — Liquid Film Data for Several Packing," *Trans. AICHE* 36, 39 (1940).

14. E. L. Knoedler and C. F. Bonilla, "Vacuum Degasification of Water in a Packed Column," *Chem. Eng. Prog.*, 50(3), 125—133 (1954).

15. J. T. Chambers, *Sea Water Conversion,* Institute of Engineering Research, University of California, Berkeley, Calif., Series No. 75, Issue No. 16, Sept. 3, 1959.

16. D. M. Eissenberg, *Summary of Present Status for Design and Analysis of Vacuum Deaerators for Distillation Plants*, OSW, ORNL/TM-3454 (April 1972).

17. E. A. Rasquin, G. Lynn, and D. N. Hanson, "Vacuum Degassing of Carbon Dioxide and Oxygen from Water in Packed Columns," *Ind. Eng. Chem., Fund.* 16(1) (1977).

18. T. H. Chilton and A. P. Colburn, *Ind. Eng. Chem.* 27, 255 (1935).

APPENDIX

Calculation of Air Leakage Rate

Total volume of desorption test section and piping system under the vacuum is as follows:

V_1 = test section volume;

V_2 = 4-in. piping volume, 6.5 ft at the top and 2 ft at the bottom of the test section;

V_3 = 1.5-in. piping volume;

$$V_1 = A_1h_1 = \frac{\pi}{4}\left[\left(\frac{11}{12}\right)^2 \text{ ft}^2\right](6 \text{ ft}) = 3.96 \text{ ft}^3;$$

$$V_2 = A_2h_2 = \frac{\pi}{4}\left[\left(\frac{4}{12}\right)^2 \text{ ft}^2\right](8.5 \text{ ft}) = 0.742 \text{ ft}^3;$$

$$V_3 = A_3h_3 = \frac{\pi}{4}\left[\left(\frac{1.5}{12}\right)^2 \text{ ft}^2\right](5 \text{ ft}) = 0.061 \text{ ft}^3;$$

$$\Sigma V = V_1 + V_2 + V_3 = 3.96 + 0.742 + 0.061 = 4.763 \text{ ft}^3.$$

Using the ideal gas law to calculate the numbers of air mole transferred from the test section to the atmosphere, when subscript 1 is vacuum and subscript 2 is atmosphere,

$$\therefore n_2 = \frac{P_2V_2}{RT_2} = \frac{(1 \text{ atm})(4.763 \text{ ft}^3)}{\left(\frac{1.31 \text{ atm-ft}^3}{°\text{K-mole}}\right)(298 \text{ K})} = 0.0122 \text{ mole} .$$

A total of 82 h was required for the gauge pressure of the test section to drop from 72.85 to 31.75 cm Hg:

P_1 abs = 76 − 72.85 = 3.15 cm Hg ;

P_2 abs = 76 − 31.75 = 44.25 cm Hg ;

$$\frac{P_1}{P_2} = \frac{n_1}{n_2} \text{ or } \frac{3.15}{44.25} = \frac{n_1}{0.0122} ;$$

n_1 = 0.0009 ;

$\Delta n = n_2 - n_1 = 0.0122 - 0.0009 = 0.0113$;

$$m = (M)\ (\Delta Pn) = (29)\ (0.0113) = 0.328\ \text{lb}\ ;$$

$$\text{Leakage rate} = \frac{0.328\ \text{lb}}{82\ \text{h}} = 0.004\ \text{lb/h}\ .$$

ORNL/TM-7438/V1
Dist. Category UC-64

Internal Distribution

1-5. F. C. Chen
6. D. M. Eissenberg
7-11. A. Golshani
12. R. E. Goodson
13. J. D. Griffin
14. H. W. Hoffman
15. S. I. Kaplan
16. T. R. La Porte
17. R. L. Linkous
18. R. N. Lyon
19. S. A. Reed
20. J. L. Rich
21. D. J. Rose
22. V. K. Smith
23. H. E. Trammell
24. ORNL Patent Office
25. Central Research Library
26. Document Reference Section
27-28. Laboratory Records Department
29. Laboratory Records (RC)

External Distribution

30. K. R. Weisbrod, Dept. of Chemical Engineering, The University of Illinios, Champaign, IL
31. C. E. Wicks, Dept. of Chemical Engineering, Oregon State University, Corvallis, OR 97331
32. S. Baron, Burns and Roe, Inc., 700 Kinderkamack Rd. Oradell, NJ 07649
33. J. J. McKetta, Dept. of Chemical Engineering, University of Texas, Austin, TX 78712
34. C. Zener, Dept. of Physics, Carnegie-Mellon University, 5000 Forbes Ave., Pittsburgh, PA 15213
35. S. L. Ridgeway, R&D Associates, 4640 Admiralty Way, P.O. Box 9695, Marina del Rey, CA 90291
36. M. I. Kay, Center for Energy and Environmental Research, University of Puerto Rico, College Station, Mayagüez, Puerto Rico 00708
37. L. A. Spielman, Dept. of Civil/Chemical Engineering, University of Delaware, Newark, DE 19711
38. A. F. Charwat, Dept. of Mechanics and Structures, University of California, 5731 Boelter Hall, Los Angeles, CA 90025
39. G. B. Wallis, School of Engineering, Dartmouth College, Hanover, NH 03755
40. A. E. Molini, Chemical Engineering Dept., Carnegie-Mellon University, 5000 Forbes Ave., Pittsburgh, PA 15213
41. S. Gronich, Program Manager, Ocean Systems Branch, Department of Energy, 600 E. St., NW, Washington, DC 20585
42. E. H. Kinelski, Program Manager, Department of Energy, 600 E. St., NW, Washington, DC 20585
43. D. H. Johnson, Solar Energy Research Institute, 1536 Cole Blvd., Golden, CO 80401
44. D. C. Kung, Technical Management Branch, Chicago Operations and Regional Office, DOE, 9800 South Cass Ave., Argonne, IL 60439

45. F. Herbaty, Technical Management Branch, Chicago Operations and Regional Office, DOE, 9800 South Cass Ave., Argonne, IL 60439
46. T. R. Penney, Solar Energy Research Institute, 1536 Cole Blvd., Golden, CO 80401
47. T. Fort, Department of Chemical Engineering, Carnegie-Mellon University, 5000 Forbes Ave., Pittsburgh, PA 15213
48. J. W. Rushing, DOE, Oak Ridge Operations, Oak Ridge, TN 37830
49. L. Wechsler, Chief Engineer, Hydronautics, Inc., Pindell School Rd., Laurel, MD 20810
50. W. Hahn, Office of Water Research and Technology, Department of Interior, Washington, DC 20240
51. K. F. Read, U.S. Naval Academy, Annapolis, MD 21402
52. L. J. Thibodeaux, Dept. of Chemical Engineering, University of Arkansas, Fayetteville, AR 72701
53. Office of Assistant Manager for Energy Research and Development, DOE, ORO, Oak Ridge, TN 37830

54-453. Given distribution as shown in DOE/TIC-4500 under category UC-64 (Ocean Energy Systems)